# Chapter 3
# Synthesis and Characterization

## *3.1 Synthesis of up-conversion phosphors*

As discussed in the section of Chapter 1, there are certain trivalent rare earth activated phosphors, which emit intense visible luminescence under near infrared light excitation. This process of upconversion is known to have its infrared to visible light conversion efficiency to be strongly dependent on the choice of host materials and the concentration of the activator as well as sensitizer. Several host materials have been used to synthesize such upconversion system. Several pairs of activator – sensitizer have been also tried. Halides of rare earth and alkaline earth metals have been the most common choice for host materials, traditionally. Several rare earth trivalent ions have been commonly used as activators and sensitizer which includes $Dy^{3+}$, $Er^{3+}$, $Ho^{3+}$, $Pr^{3+}$, $Tm^{+3}$ and $Yb^{3+}$.

In the present study a set of new host materials namely Lanthanum Molybdate, Bismuth Oxide and Cadmium Oxide have been used to synthesize up-conversion phosphors with Erbium ($Er^{3+}$) and Ytterbium ($Yb^{3+}$) as activator and sensitizer respectively.

1. $La_2(MoO_4)_3$ : Yb, Er
2. $Bi_2O_3$ : Yb, Er
3. CdO : Yb, Er

All these materials have been doped by $Er^{3+}$ as activator and $Yb^{3+}$ as sensitizer. While a host of chemical methods can be used for synthesis, the samples in this work were prepared using the simple and inexpensive method of precipitation.

### *3.1.1 Synthesis of $La_2(MoO_4)_3$: $Yb^{3+}$, $Er^{3+}$ up-conversion phosphor*

Samples of $La_2(MoO_4)_3$: Yb, Er were synthesized using the precipitation method. The process followed is as under.

Stoichiometric amount of Lanthanum Oxide ($La_2O_3$), Ytterbium Oxide ($Yb_2O_3$) and Erbium Oxide ($Er_2O_3$) were taken and dissolved in 10 ml of dilute $HNO_3$ to prepare Solution A. The solution was heated moderately to drive away the unreacted $HNO_3$. The residue obtained was dissolved in 30 ml of deionised water and stirred for one hour at room temperature.

Another mixture (Solution B) was prepared by dissolving stoichiometric amount of Ammonium Molybdate Oxide ($(NH_4)_6Mo_7O_{24}$) in 30 ml of deionised water and stirring it for one hour at room temperature.

Solution A was added to Solution B drop by drop with continuous stirring. The mixture was then stirred continuously for 24 hours. Gradually, the precipitates were formed. These precipitates were then centrifuged at 3000 rpm for 15 minutes. The residual precipitates were washed twice in deionised water and dried. The color of the precipitates was light green like that of bottle guard. This powder was then heated at 800 ºC for 5 hours and then cooled. The final product was a lemon colored powder.

Three samples were synthesized in the following proportion of the host metal, the sensitizer and activator.

| | |
|---|---|
| LMO 1 | ( $La_{79}$ : $Yb_{20}$ : $Er_1$ ) |
| LMO 2 | ( $La_{78}$ : $Yb_{20}$ : $Er_2$ ) |
| LMO 3 | ( $La_{77}$ : $Yb_{20}$ : $Er_3$ ) |

The samples were subjected to EDAX analysis to confirm the presence of elements, particularly the doped elements in the samples LMO 1, LMO 2 and LMO 3 as shown in figure 3.1, 3.2 and 3.3 respectively. The results confirm the presence of all the elements involved.

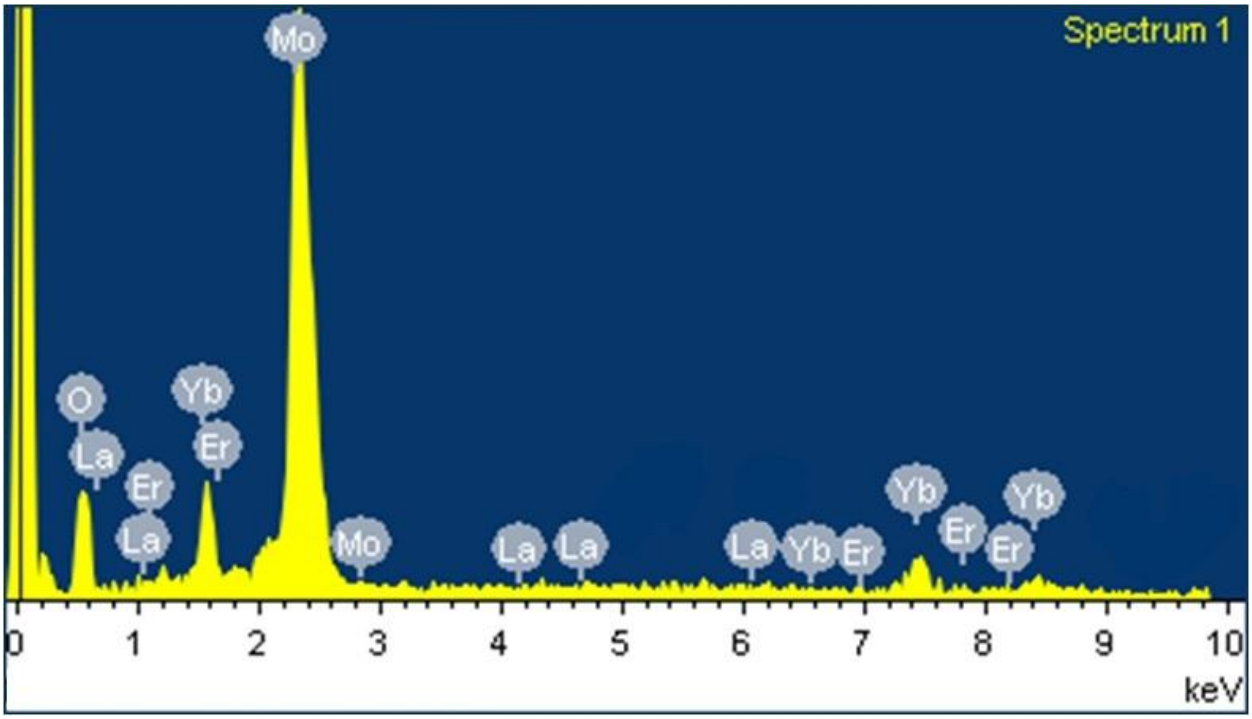


Figure 3.1: EDAX spectra of LMO 1

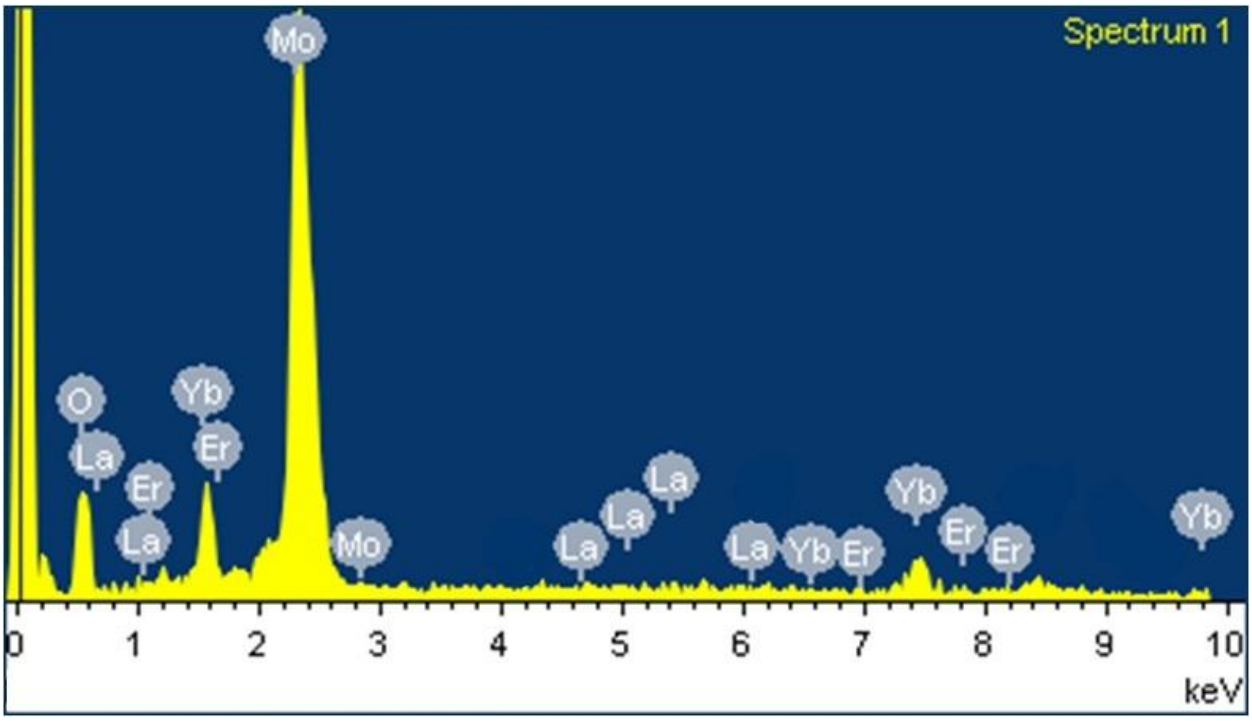


Figure 3.2: EDAX spectra of LMO 2

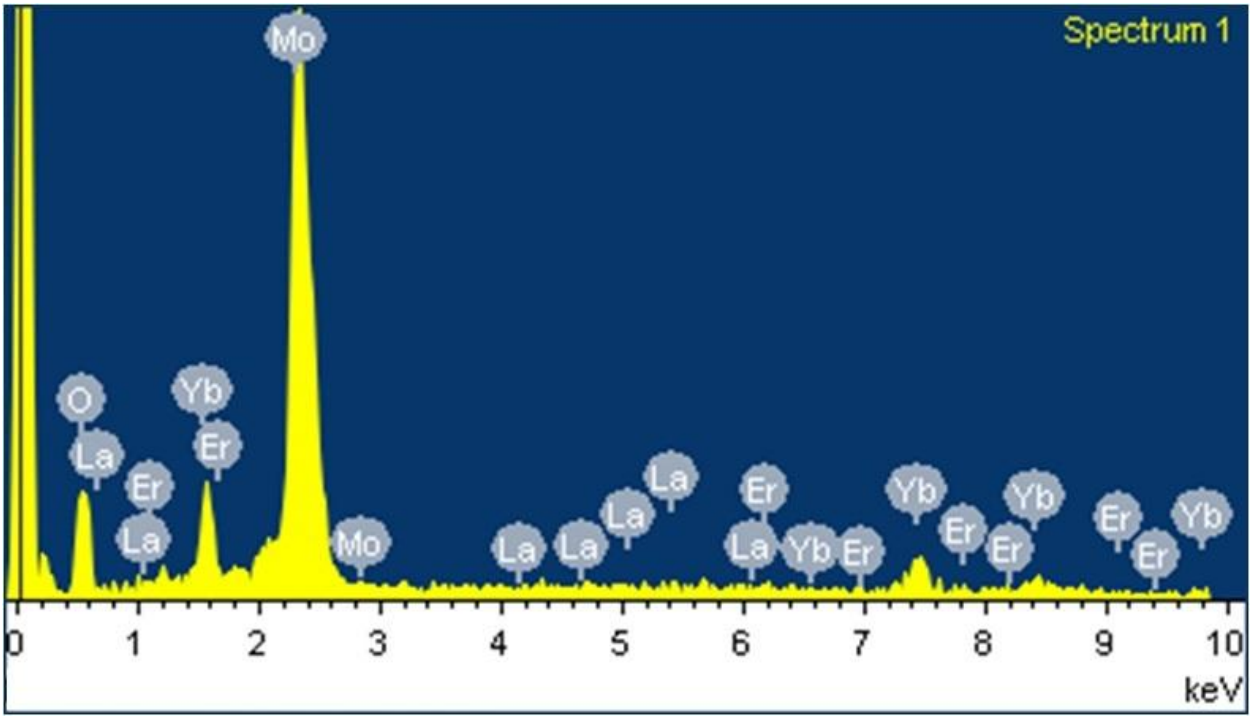


Figure 3.3: EDAX spectra of LMO 3

### *3.1.2 Synthesis of $Bi_2O_3$: $Yb^{3+}$, $Er^{3+}$ up-conversion phosphor*

Stoichiometric amount of Bismuth Nitrate [$Bi(NO_3)_3$], Ytterbium Nitrate [$Yb(NO_3)_3$] and Erbium Nitrate [$Er(NO_3)_3$] were taken and mixed in 30 ml of dilute $HNO_3$. More $HNO_3$ was added with stirring till the solution became transparent. To this solution, 20 ml of polyethylene glycol (PEG 400) was added as dispersant with continuous stirring. Another 50 ml solution of 4 mol/lit NaOH was poured into the above solution which resulted into the formation of yellow precipitates. The solution with precipitates was heated at 90º C for two hours with continuous stirring and then cooled down to room temperature. The precipitates were filtered, washed with alcohol as well as deionised water several times and then dried. The final product was a light yellow powder.

Three samples were synthesized in the following proportion of the host material, sensitizer and activator.

BO 1 ( $Bi_{79} : Yb_{20} : Er_1$ )

BO 2 ( $Bi_{78} : Yb_{20} : Er_2$ )

BO 3 ( $Bi_{77} : Yb_{20} : Er_3$ )

The samples were subjected to EDAX analysis to confirm the presence of elements, particularly the doped elements in the samples BO 1, BO 2 and BO 3 as shown in figure 3.4, 3.5 and 3.6 respectively. The results confirm the presence of all the elements involved.

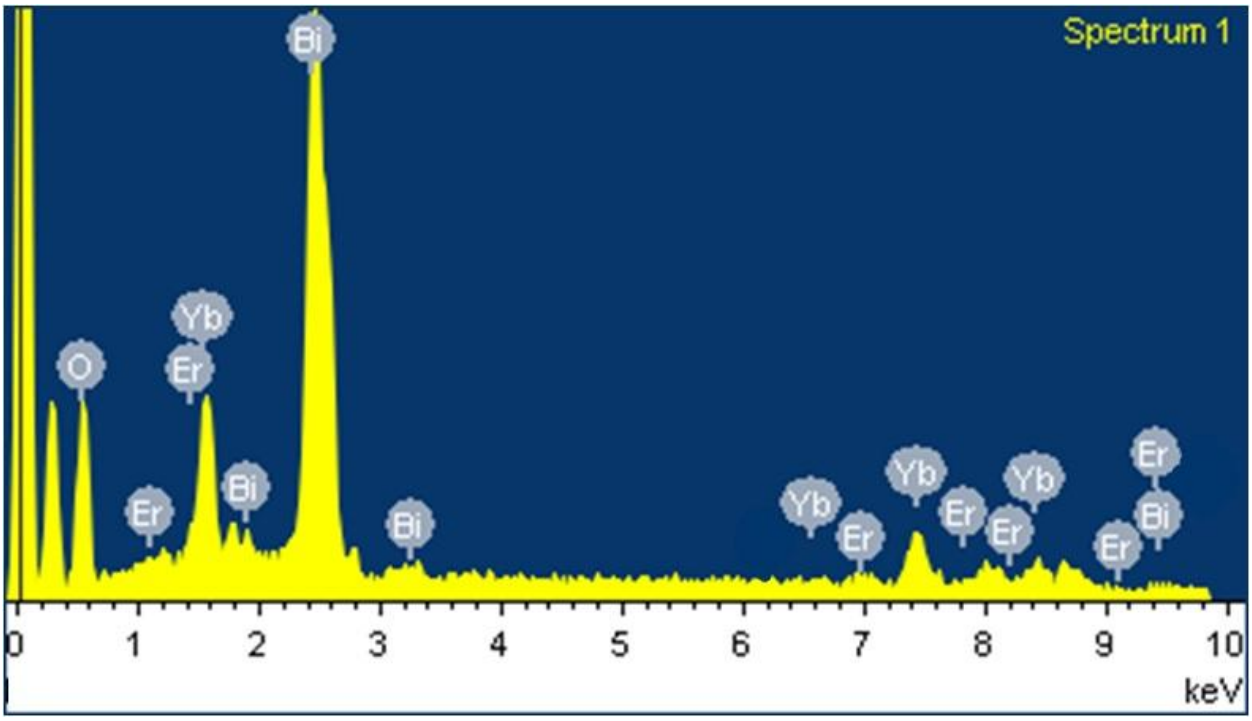


Figure 3.4: EDAX spectra of BO 1

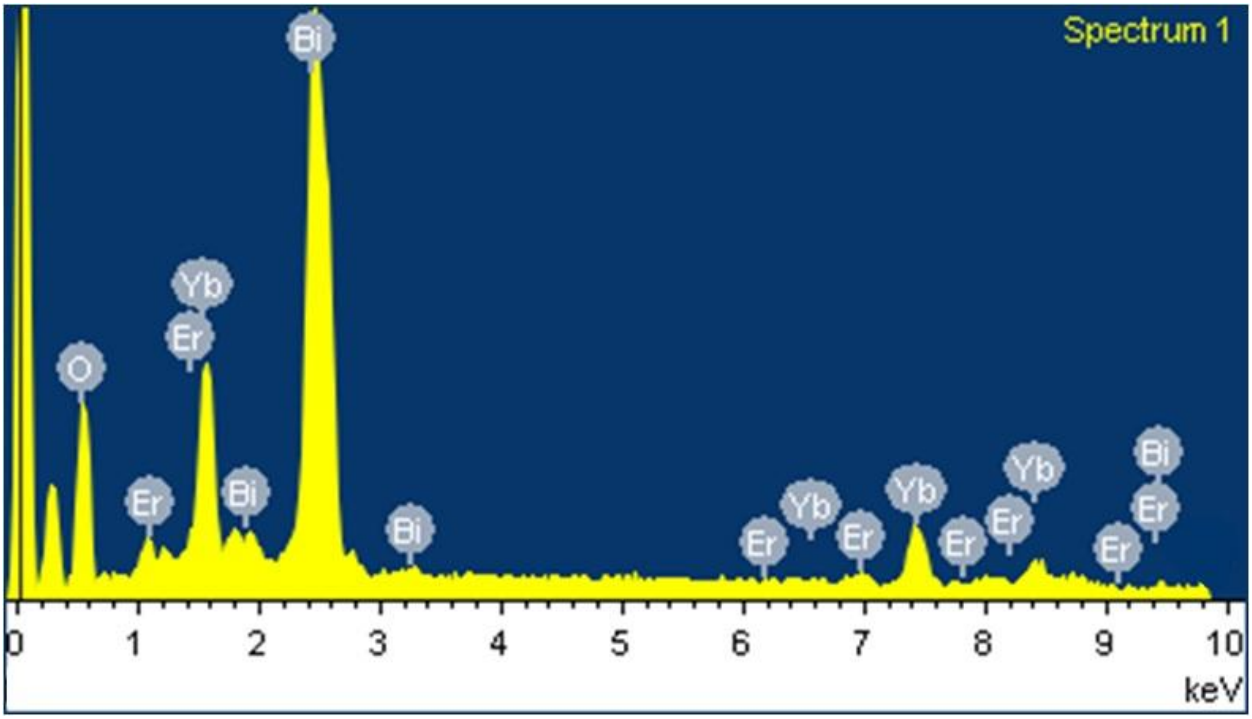


Figure 3.5: EDAX spectra of BO 2

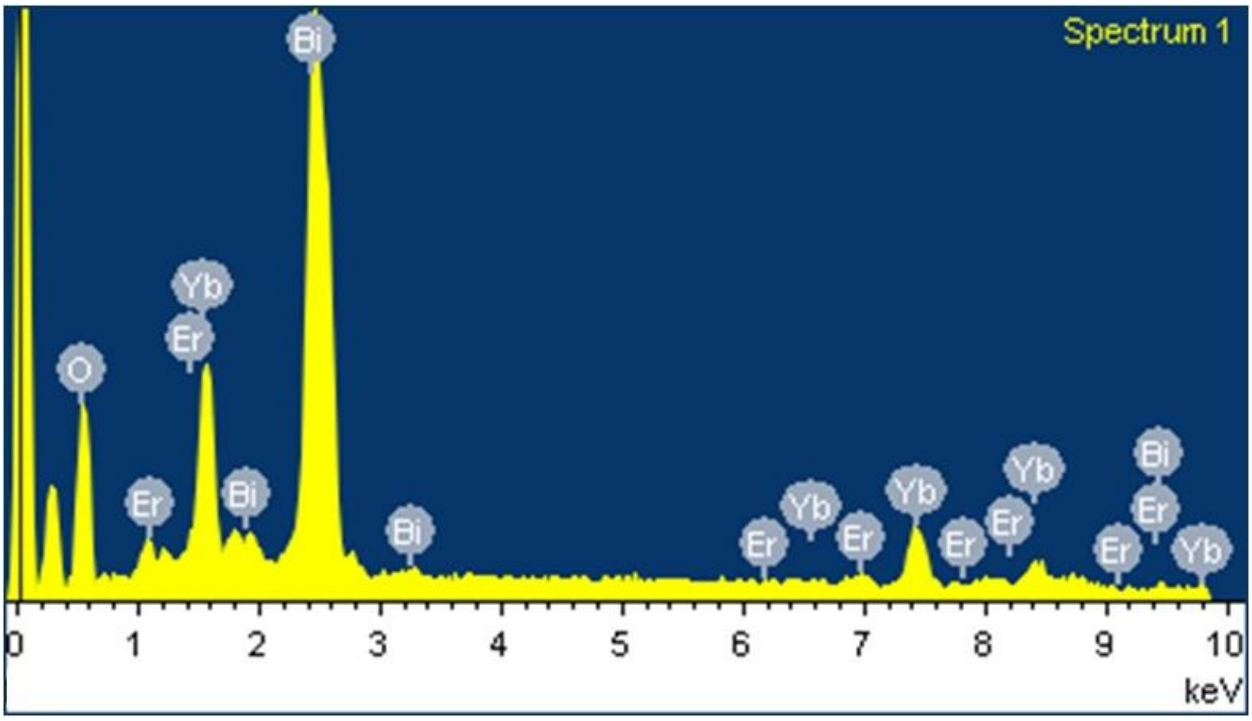


Figure 3.6: EDAX spectra of BO 3

### *3.1.3 Synthesis of CdO: $Yb^{3+}$, $Er^{3+}$ up-conversion phosphor*

Stoichiometric amount of $CdCl_2$ was dissolved in 50 ml of Ethanol and stirred for 30 minutes at room temperature to prepare Solution A.

Another Solution B was prepared by dissolving stoichiometric amount of $Yb_2O_3$ and $Er_2O_3$ in concentrated Hydrochloric acid (HCl).

The solution B was added to solution A with continuous stirring for 10 minutes at room temperature. Aqueous solution of NaOH was added to this mixture with continuous stirring to maintain a pH value of 10. Subsequently, the solution was kept for 10 hours for deposition of precipitates. These precipitates were collected and dried at 100º C for two hours. White colored powder was obtained. This powder was heated at 400º C for one hour, which resulted into a brownish powder.

These samples were synthesized in the following proportion of the host metal, sensitizer and activator.

CO 1 ( $Cd_{79}$ : $Yb_{20}$ : $Er_1$ )

CO 2 ( $Cd_{78}$ : $Yb_{20}$ : $Er_2$ )

CO 3 ( $Cd_{77}$ : $Yb_{20}$ : $Er_3$ )

The samples were subjected to EDAX analysis to confirm the presence of elements, particularly the doped elements in the samples CO 1, CO 2 and CO 3 as shown in figure 3.7, 3.8 and 3.9

respectively.. The results confirm the presence of all the elements involved, except in the case of sample CO1 which does not show the presence of Erbium (Er). This shows that Er has not been incorporated in the material.

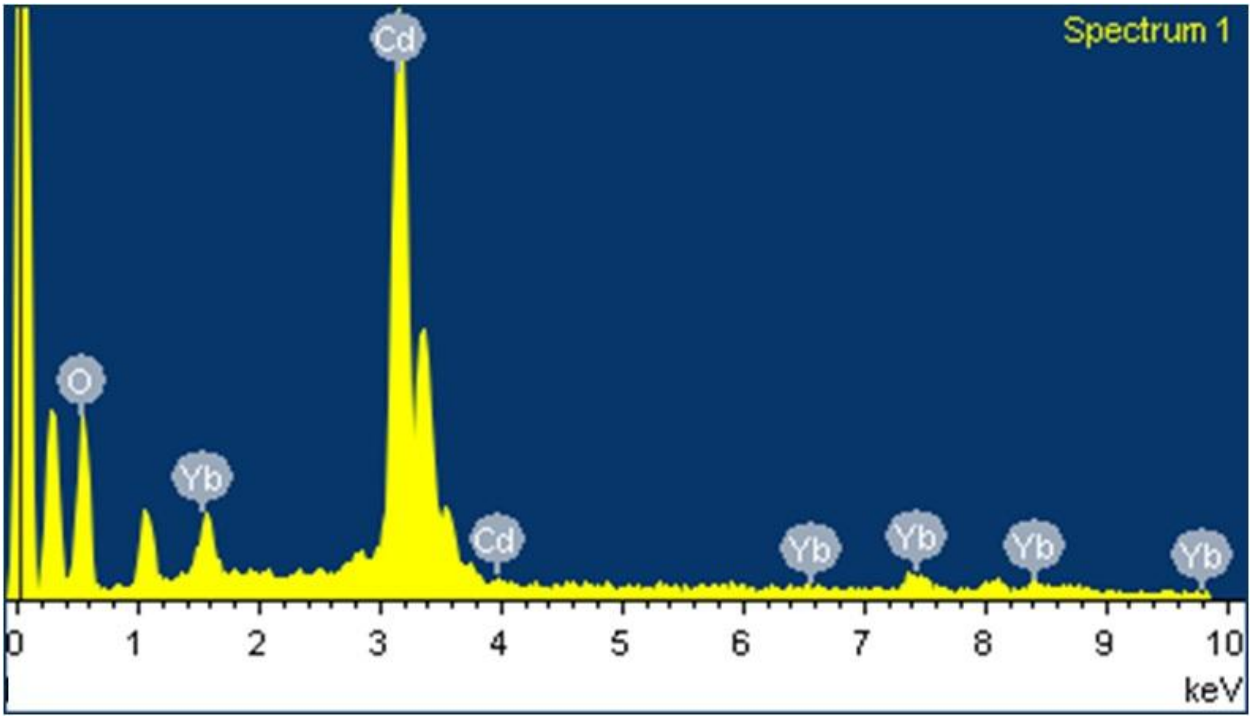


Figure 3.7: EDAX spectra of CO 1

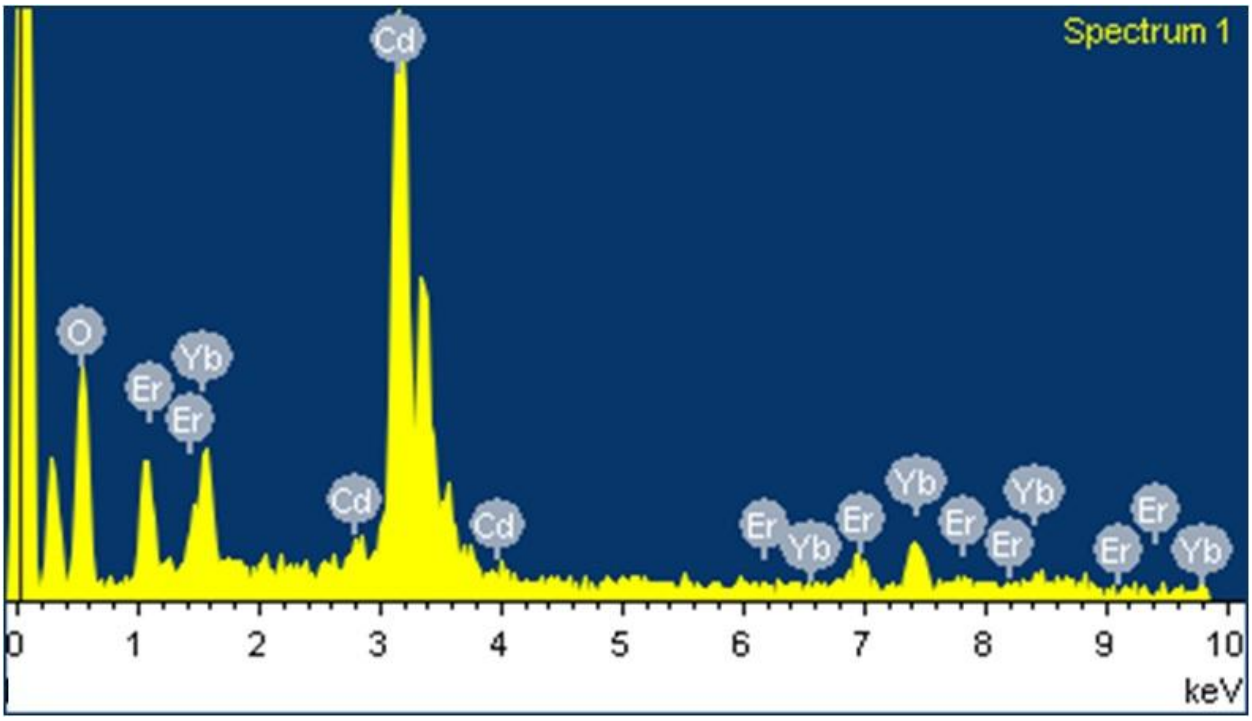


Figure 3.8: EDAX spectra of CO 2

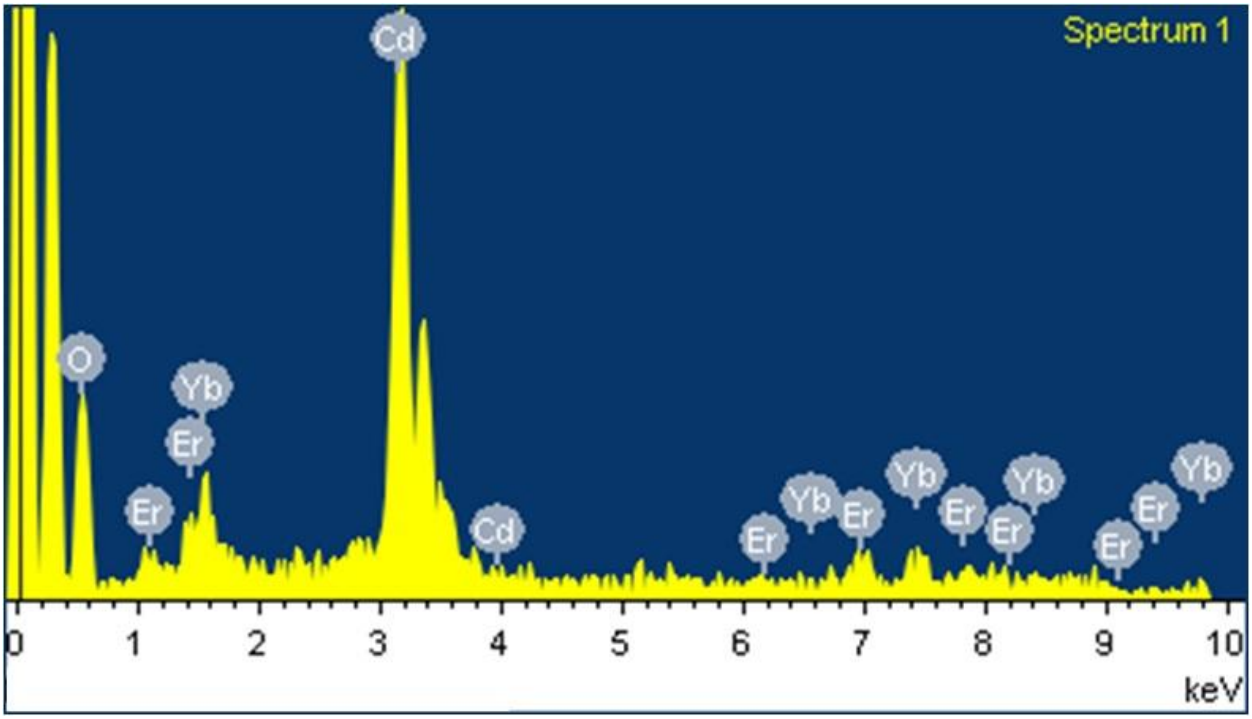


Figure 3.9: EDAX spectra of CO 3

## *3.2 Characterization of materials*

Characterization of the materials gives the detailed information about the synthesized materials. Here, all the synthesized phosphors were characterized by X – ray powder diffraction (XRD), Scanning electron microscopy (SEM) and Energy dispersive X – ray spectroscopy (EDAX).

It gives information about the size, structure, phase, surface topography, elemental composition and about the presence of the functional groups, bonds etc. in the synthesized materials.

### *3.2.1 XRD Analysis*

The X-ray powder diffraction technique has been used to get information regarding the structural properties like phase and crystallite size of the material.

#### *1) $La_2(MoO_4)_3$: $Yb^{3+}$, $Er^{3+}$*

Figure 3.10 shows the XRD pattern for sample LMO 1 ($La_2(MoO_4)_3$:$Yb^{3+}$, $Er^{3+}$), which has sharp peaks. The pattern indicates high degree of crystallinity. These peaks can be ascribed to $La_2(MoO_4)_3$. The structure is predominantly in monoclinic phase. The peak at 2Θ value of 25.85º has the highest intensity, which is the characteristic peak of (-421) plane. d-values of majority of the peaks match with those reported in the JCPDS file (70 – 1382 for $La_2(MoO_4)_3$), while a few vary marginally with the respective peaks in the same file. That can be attributed to the presence of dopants.

Figure 3.11 gives the pattern for sample LMO 2, which is identical to the pattern of sample LMO 1. This pattern also indicates high degree of crystallinity. The peak at 2Θ value of 25.85º has the highest intensity. d-values of the peaks match with JCPDS file 70 – 1382 for $La_2(MoO_4)_3$.

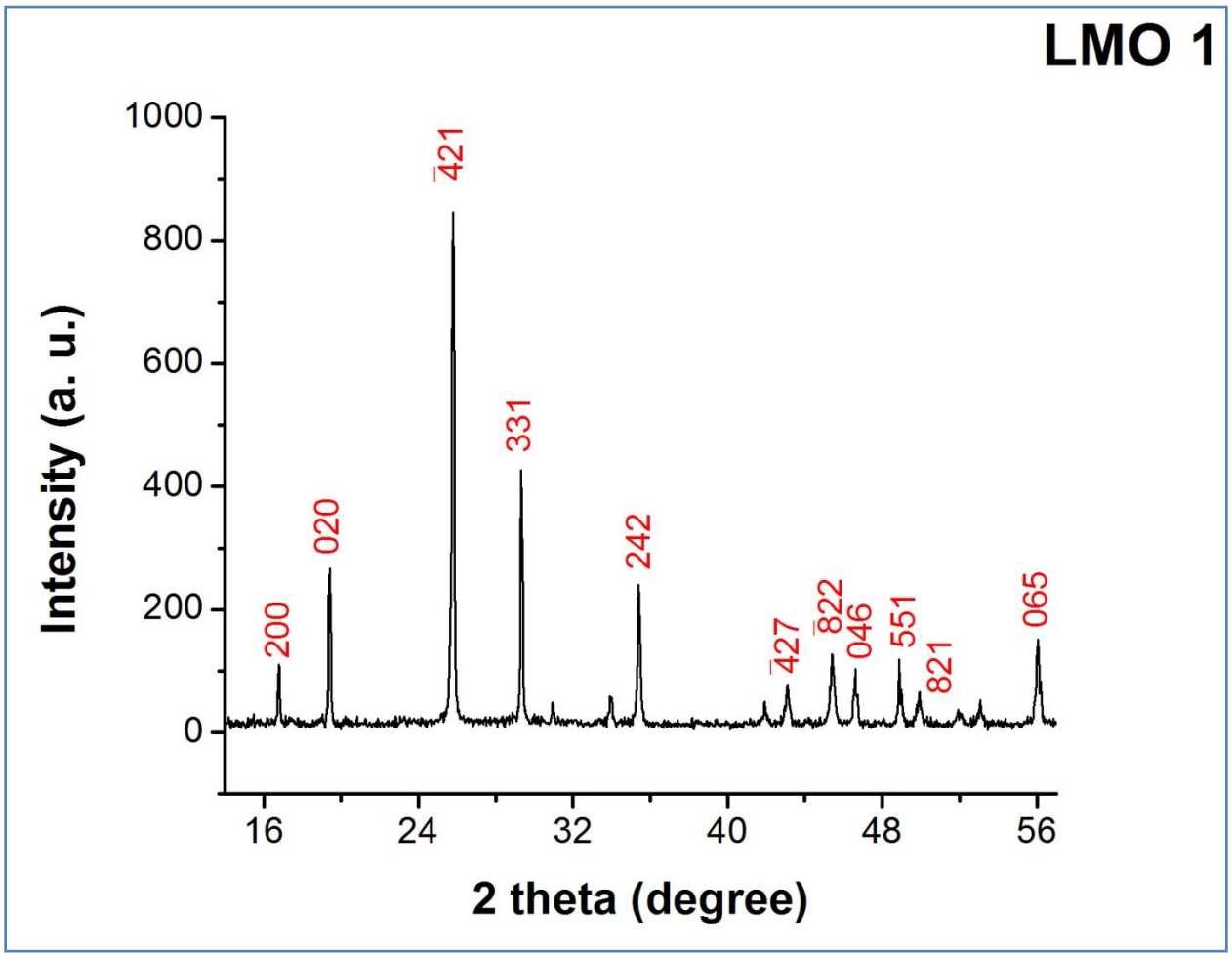


Figure 3.10: XRD pattern of $La_2(MoO_4)_3$ phosphors doped with Yb and Er for LMO 1

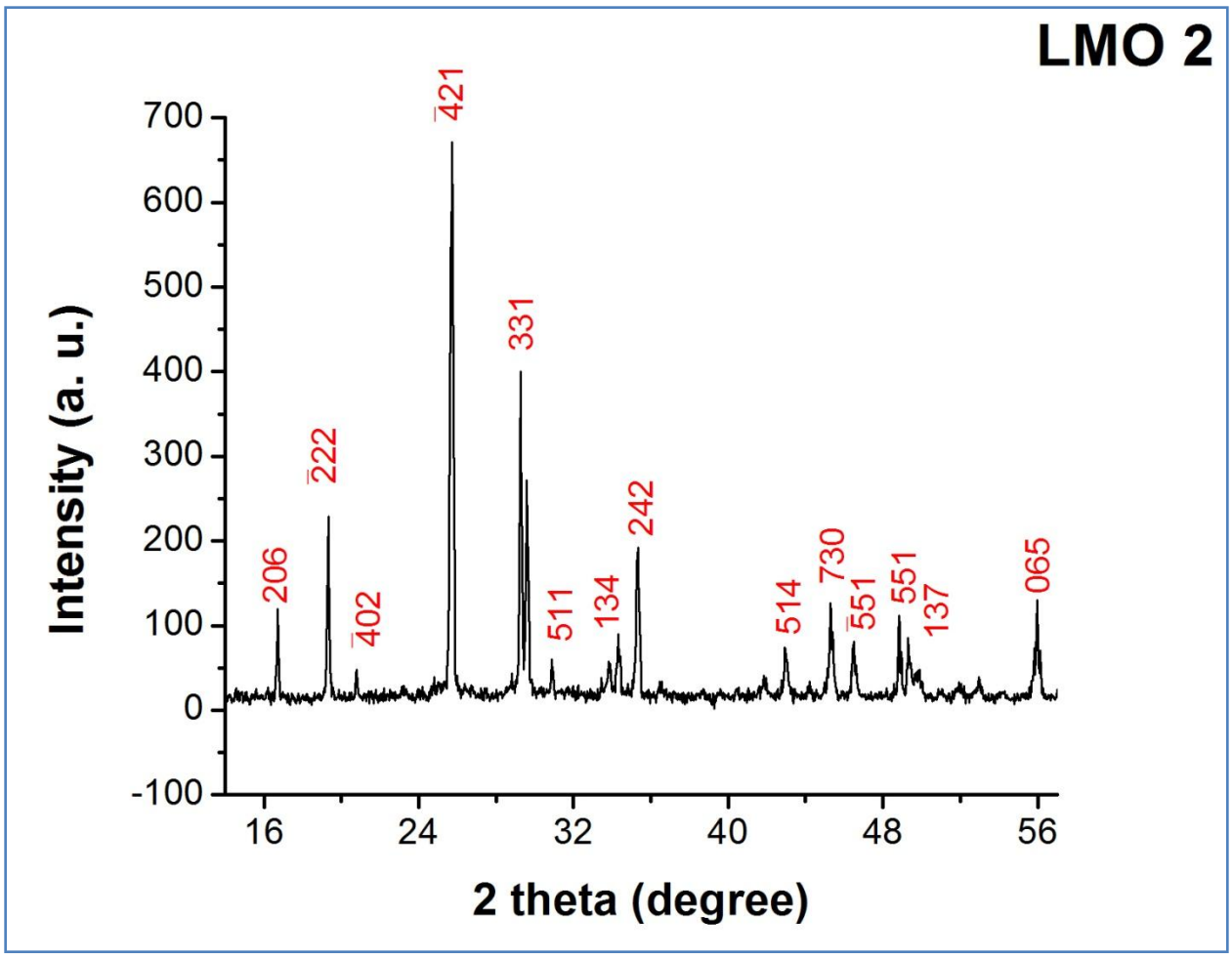


Figure 3.11: XRD pattern of $La_2(MoO_4)_3$ phosphors doped with Yb and Er for LMO 2

Figure 3.12 shows the pattern for sample LMO 3 which is again similar to the earlier two samples. The peak at 2Θ values of 25.85º has the highest intensity. d-value of the peaks match with the JCPDS file 70 – 1382 for $La_2(MoO_4)_3$, with few exceptions.

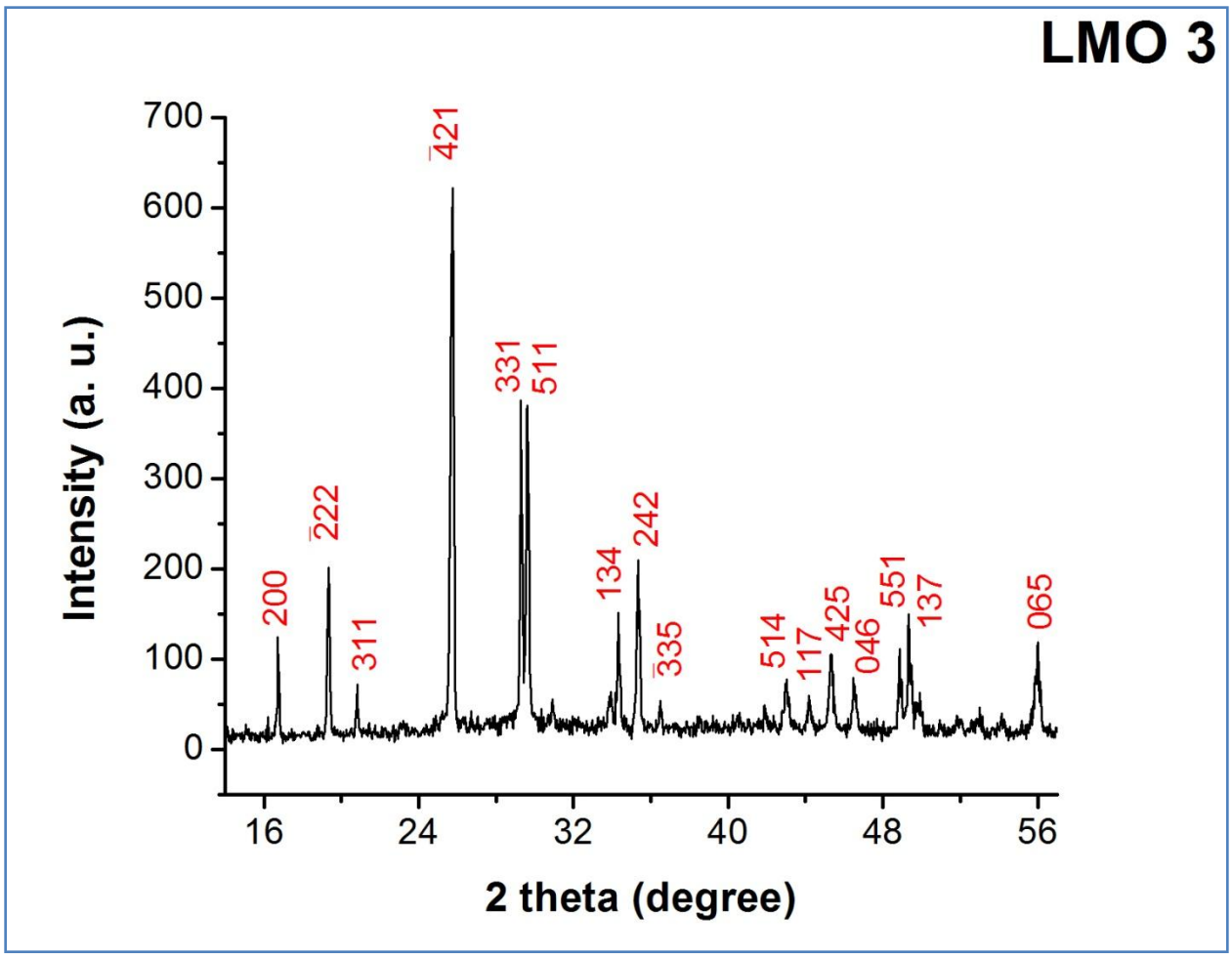


Figure 3.12: XRD pattern of $La_2(MoO_4)_3$ phosphors doped with Yb and Er for LMO 3

Comparison of standard d-values of JCPDS file no. 70-1382 with the calculated d-values of the samples are given in table 3.1. The slight deviation from the standard values can be attributed to the presence of activator and co-activator.

| **d – values JCPDS file no. 70 - 1382** | **d – values (Calculated)** | | | | | |
|---|---|---|---|---|---|---|
| | **Sample LMO 1** | **hkl** | **Sample LMO 2** | **hkl** | **Sample LMO 3** | **hkl** |
| 4.4606 | 4.5676 | -222 | 4.5613 | -222 | 4.5721 | -222 |
| 4.3203 | --- | --- | --- | --- | 4.3023 | 311 |
| 3.4607 | 3.4424 | -421 | 3.4333 | -421 | 3.4385 | -421 |
| 3.0209 | 3.0384 | 331 | 3.0557 | 331 | 3.0303 | 331 |
| 2.8844 | 2.8876 | 511 | 2.8849 | 511 | 2.8876 | 511 |
| 2.6192 | 2.6321 | 134 | 2.6146 | 134 | 2.6112 | 134 |
| 2.5415 | 2.5347 | 242 | 2.5347 | 242 | 2.5319 | 242 |
| 2.4520 | --- | --- | --- | --- | 2.4607 | -335 |
| 2.1488 | 2.1476 | 244 | --- | --- | --- | --- |
| 2.1172 | --- | --- | 2.1070 | 514 | 2.1056 | 514 |
| 2.0952 | 2.0953 | -427 | --- | --- | --- | --- |
| 2.0452 | --- | --- | --- | --- | 2.0475 | 117 |
| 2.0076 | --- | --- | --- | --- | 2.0015 | 425 |
| 1.9987 | 1.9986 | -822 | --- | --- | --- | --- |
| 1.9959 | --- | --- | 1.9940 | 730 | --- | --- |
| 1.9517 | --- | --- | 1.9510 | -551 | --- | --- |
| 1.9369 | 1.9323 | 046 | --- | --- | 1.9321 | 046 |
| 1.8627 | 1.8610 | 551 | 1.8625 | 551 | --- | --- |
| 1.8409 | --- | --- | 1.8472 | 137 | 1.8461 | 137 |
| 1.8295 | 1.8216 | 821 | --- | --- | --- | --- |
| 1.7255 | 1.7256 | 714 | --- | --- | --- | --- |
| 1.6928 | --- | --- | 1.6992 | 156 | --- | --- |
| 1.6692 | 1.6406 | 065 | 1.6433 | 065 | 1.6425 | 065 |

Table 3.1: Comparison of standard d-values of JCPDS file no. 70-1382 with the calculated d-values of the samples of $La_2(MoO_4)_3$ phosphors

Some peaks match with JCPDS file no. 78 – 1691 of $Yb_2O_3$ and 76 – 0159 for $Er_2O_3$ which shows that there is some amount of residual $Yb_2O_3$ and $Er_2O_3$ in the samples.

## *2) $Bi_2O_3$: $Yb^{3+}$, $Er^{3+}$*

Figure 3.13 shows the XRD pattern for sample BO1 ($Bi_2O_3$:$Yb^{3+}$, $Er^{3+}$), which has sharp peaks. The pattern indicates high degree of crystallinity. These peaks can be ascribed to $Bi_2O_3$. The structure is monoclinic. The peak at 2Θ value of 27.37º has the highest intensity, which is the characteristic peak of (-121) plane. d-values of the peaks match with those reported in the JCPDS file 71 – 2274 for $Bi_2O_3$.

Figure 3.14 gives the pattern for sample BO2 ($Bi_2O_3$:$Yb^{3+}$, $Er^{3+}$), which is identical to the pattern of sample BO1. This pattern also indicates high degree of crystallinity. The peak at 2Θ value of 27.46º has the highest intensity. d-values of the peaks match with JCPDS file JCPDS file 71 – 2274 for $Bi_2O_3$.

Figure 3.15 shows the pattern for sample BO3 ($Bi_2O_3$:$Yb^{3+}$, $Er^{3+}$) which is again similar to the earlier two samples. The peak at 2Θ value of 27.37º corresponding to (120) plane has the highest intensity. d-value of the peaks match with the JCPDS file 71 – 2274 for $Bi_2O_3$.

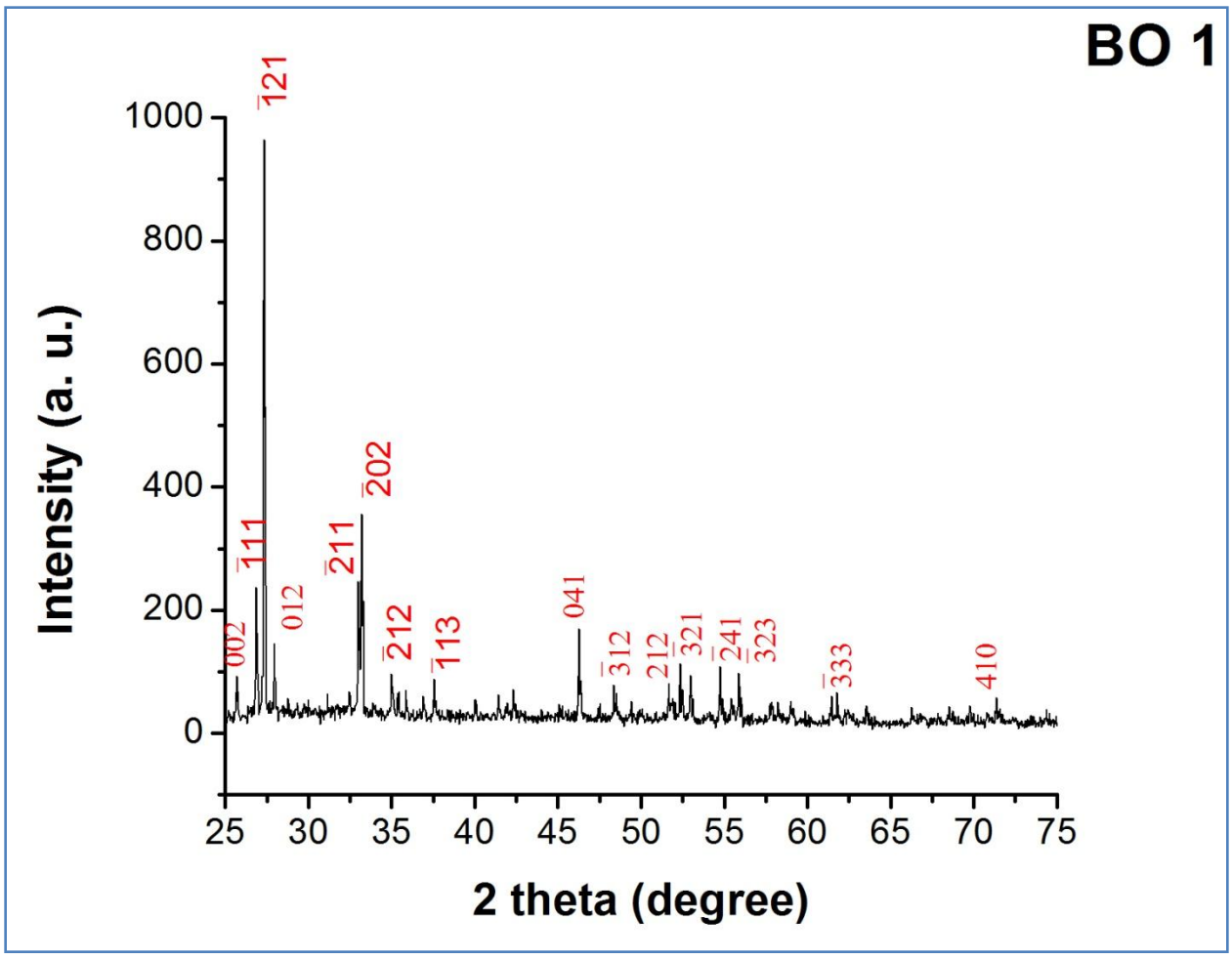


Figure 3.13: XRD pattern of $Bi_2O_3$ phosphors doped with Yb and Er (BO 1)

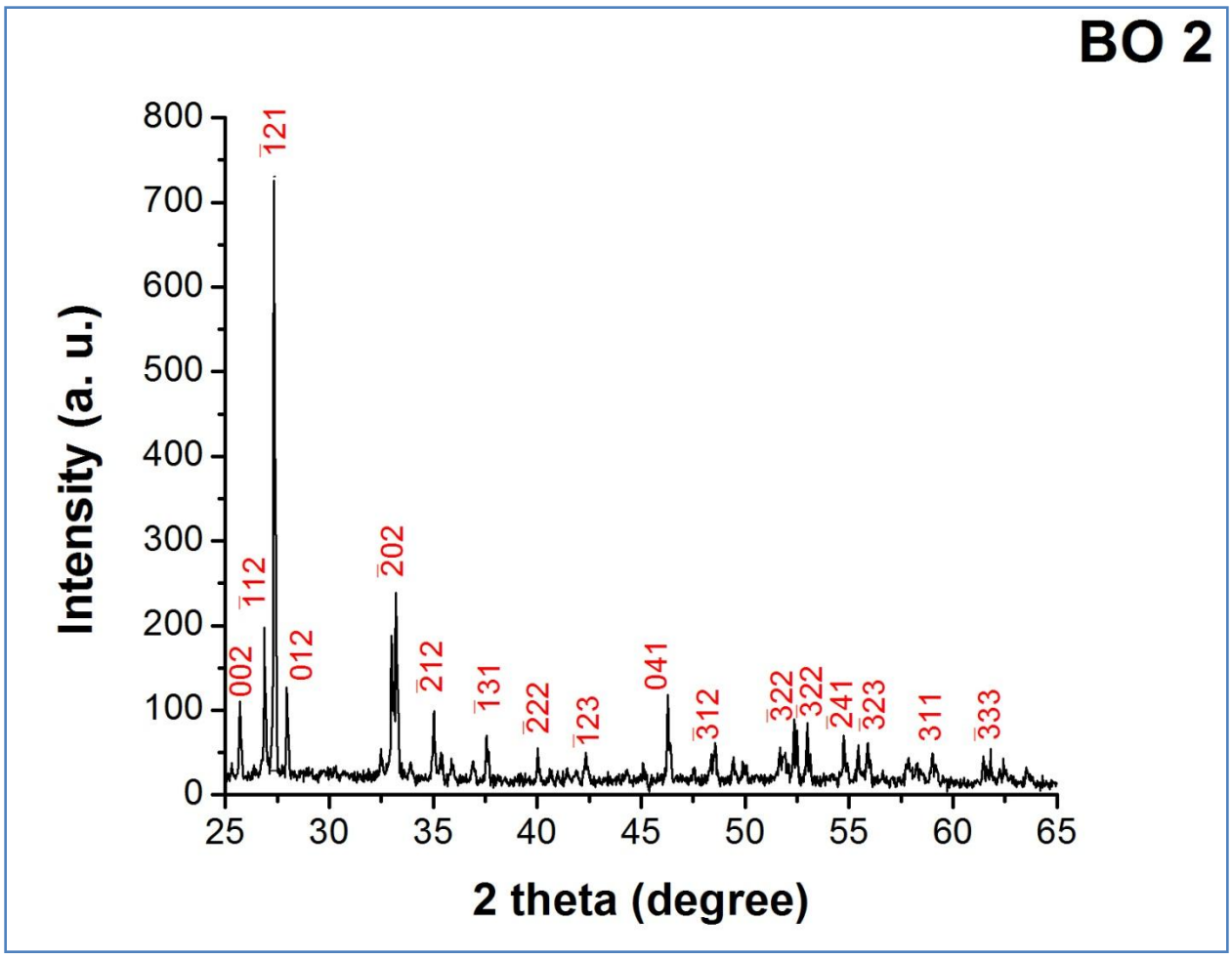


Figure 3.14: XRD pattern of $Bi_2O_3$ phosphors doped with Yb and Er (BO 2)

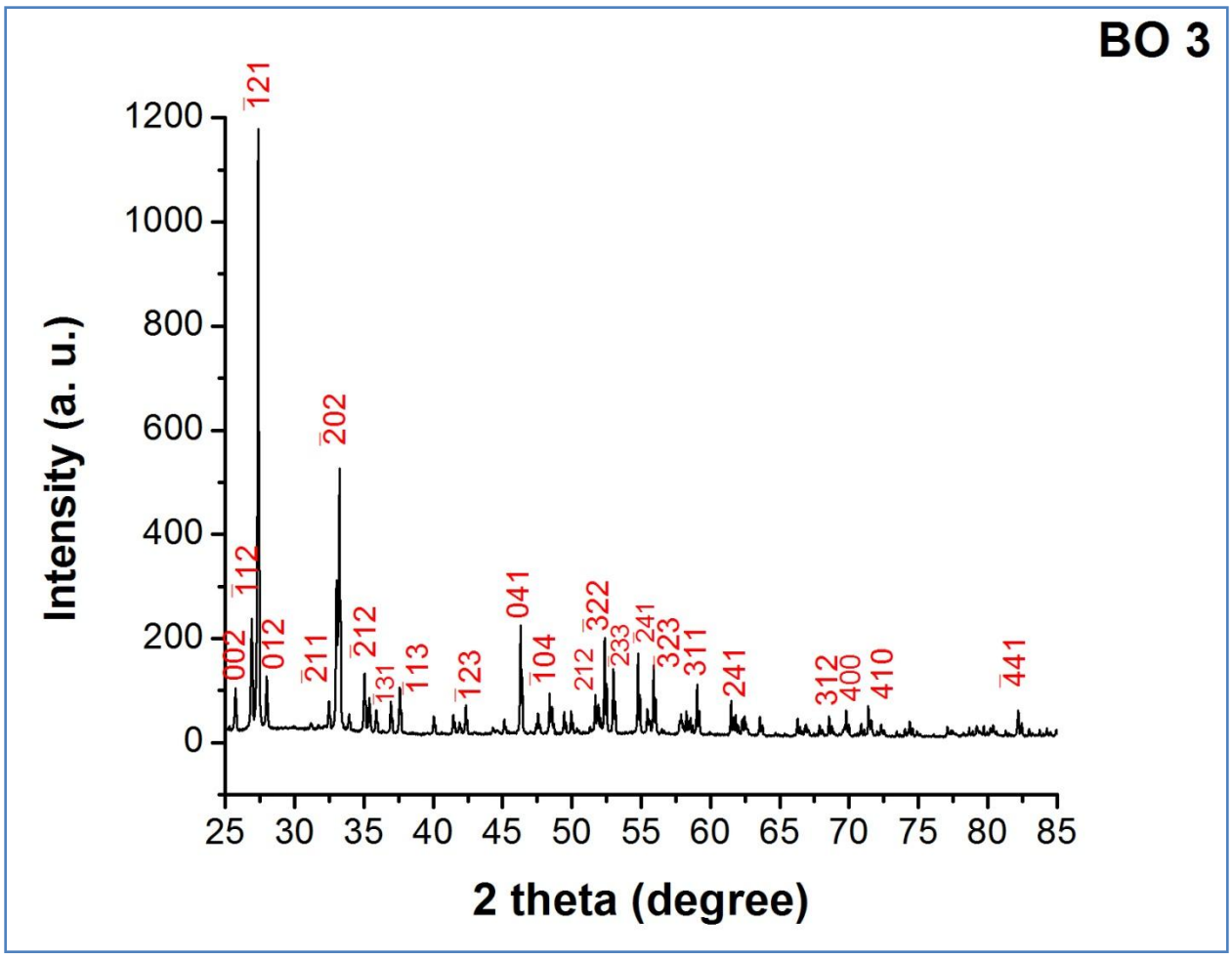


Figure 3.15: XRD pattern of $Bi_2O_3$ phosphors doped with Yb and Er (BO 3)

Comparisons of standard d-values of JCPDS file no. 71 - 2274 with the calculated d-values of the samples are given in table 3.2. The slight deviation from the standard values can be attributed to the presence of activator and co-activator.

| **d – values JCPDS file no. 71 - 2274** | **d – values (Calculated)** | | | | | |
|---|---|---|---|---|---|---|
| | **Sample B 1** | **hkl** | **Sample B 2** | **hkl** | **Sample B 3** | **hkl** |
| 3.4563 | 3.4555 | 002 | 3.4551 | 002 | 3.4595 | 002 |
| 3.3111 | 3.3144 | -112 | 3.3133 | -112 | 3.3177 | -112 |
| 3.2532 | 3.2500 | -121 | 3.2503 | -121 | 3.2523 | -121 |
| 3.1829 | 3.1839 | 012 | 3.1895 | 012 | 3.1872 | 012 |
| 2.7516 | --- | --- | --- | --- | 2.7516 | -211 |
| 2.6918 | 2.6976 | -202 | 2.6976 | -202 | 2.6973 | -202 |
| 2.5589 | 2.5570 | -212 | 2.5549 | -212 | 2.5571 | -212 |
| 2.3890 | 2.3844 | -113 | 2.3854 | -113 | 2.3873 | -113 |
| 2.2490 | --- | --- | 2.2481 | -222 | --- | --- |
| 2.1310 | --- | --- | 2.1393 | -123 | 2.1397 | -123 |
| 1.9579 | 1.9522 | 041 | 1.9505 | 041 | 1.9585 | 041 |
| 1.8790 | 1.8705 | -312 | 1.8791 | -312 | 1.8765 | -312 |
| 1.7658 | 1.7644 | 212 | --- | --- | 1.7666 | 212 |
| 1.7454 | 1.7443 | -321 | 1.7431 | -322 | 1.7490 | -322 |
| 1.7254 | --- | --- | 1.7299 | -233 | 1.7259 | -233 |
| 1.6739 | 1.6748 | -241 | 1.6799 | -241 | 1.6715 | -241 |
| 1.5628 | --- | --- | --- | --- | 1.5600 | 311 |
| 1.5060 | --- | --- | --- | --- | 1.5084 | 241 |
| 1.4993 | 1.4998 | -333 | 1.4991 | -333 | --- | --- |
| 1.3670 | --- | --- | --- | --- | 1.3653 | 312 |
| 1.3459 | --- | --- | --- | --- | 1.3459 | 400 |
| 1.3280 | 1.3200 | 410 | --- | --- | 1.3216 | 410 |
| 1.1713 | --- | --- | --- | --- | 1.1725 | -441 |

Table 3.2: Comparison of standard d-values of JCPDS file no. 71 - 2274 with the calculated d-values of the samples of $Bi_2O_3$

In this, case also, some peaks match with JCPDS file no. 78 – 1691 of $Yb_2O_3$ which shows that there is some amount of residual $Yb_2O_3$ in the samples.

## 3) *CdO: Yb, Er up-conversion phosphors*

Figure 3.16 shows the XRD pattern for sample CO 1 (CdO:$Yb^{3+}$, $Er^{3+}$), which has sharp peaks. The pattern indicates high degree of crystallinity. These peaks can be ascribed to CdO. The structure is cubic. The peak at 2Θ value of 32.95º has the highest intensity, which is the characteristic peak of (111) plane. d-values of the peaks match with those reported in the JCPDS file 75 - 0594 for CdO.

Figure 3.17 gives the pattern for sample CO 2 (CdO:$Yb^{3+}$, $Er^{3+}$), which is identical to the pattern of sample CO 1. This pattern also indicates high degree of crystallinity. The peak at 2Θ value of 32.95º has the highest intensity. d-values of the peaks match with JCPDS file 75 - 0594 for CdO.

Figure 3.18 shows the pattern for sample CO 3 (CdO:$Yb^{3+}$, $Er^{3+}$) which is again similar to the earlier two samples. The peak at 2Θ value of 32.87º corresponding to (111) plane has the highest intensity. d-value of the peaks match with the JCPDS file 75 - 0594 for CdO.

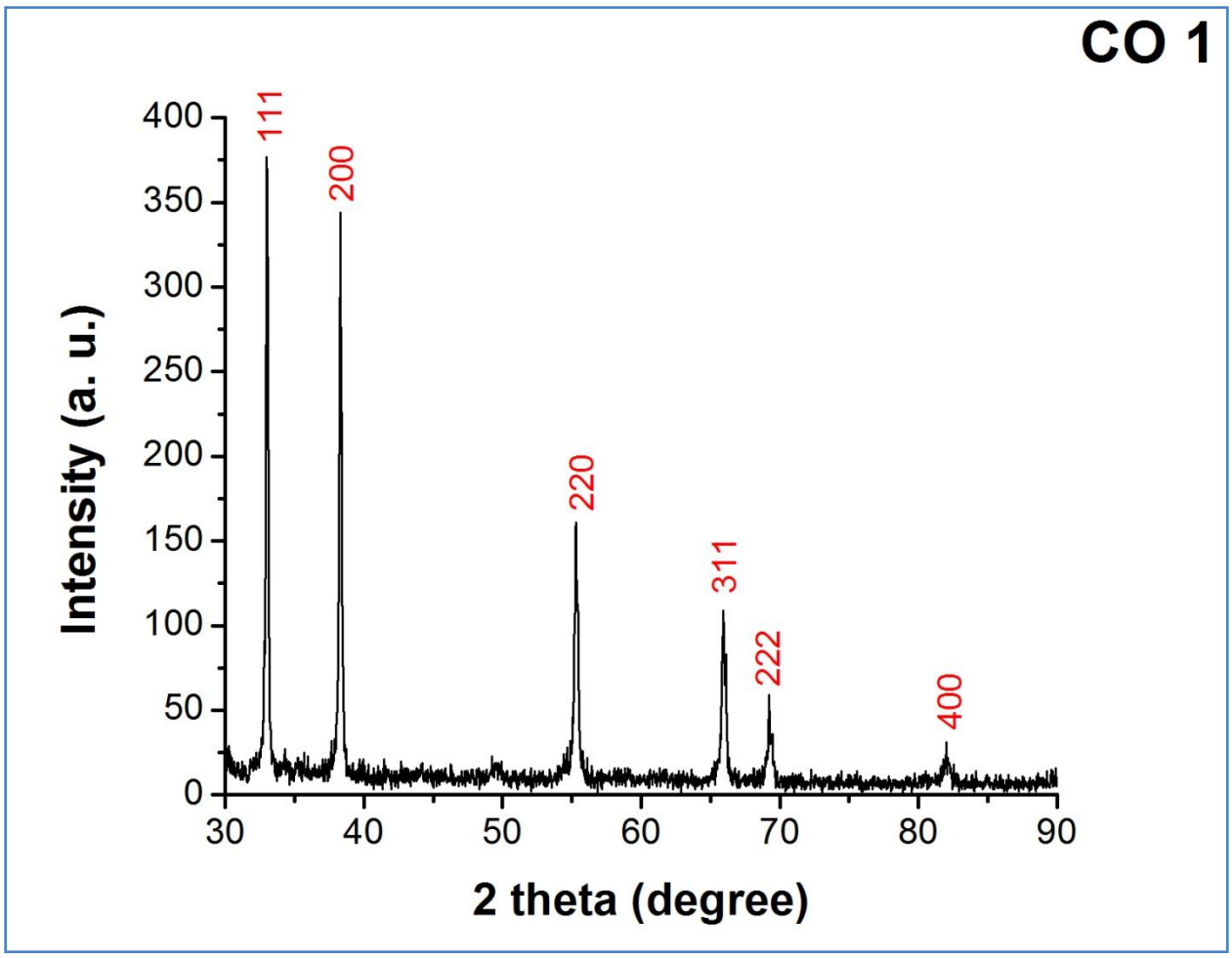


Figure 3.16: XRD pattern of CdO phosphors doped with Yb and Er (CO 1)

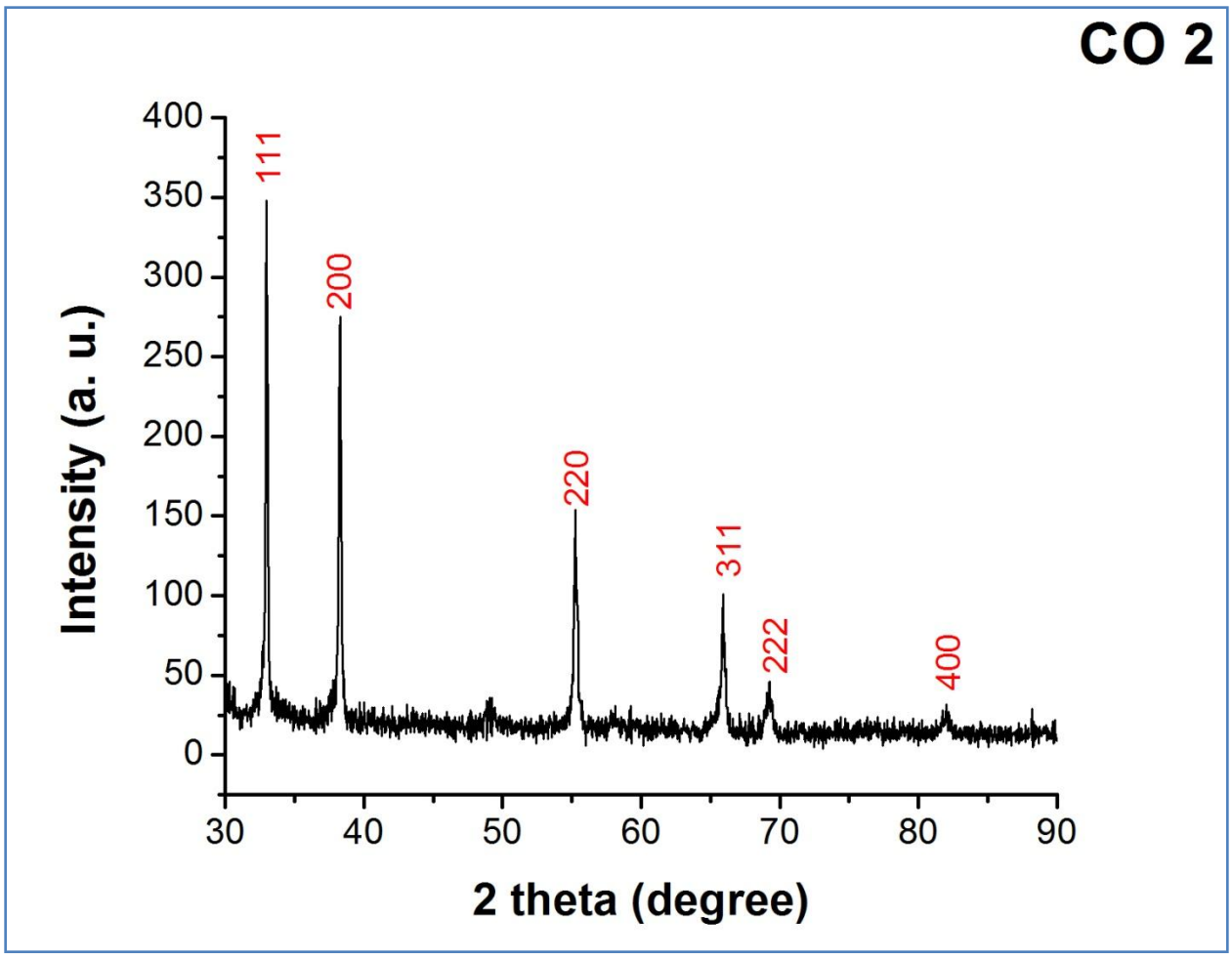


Figure 3.17: XRD pattern of CdO phosphors doped with Yb and Er (CO 2)

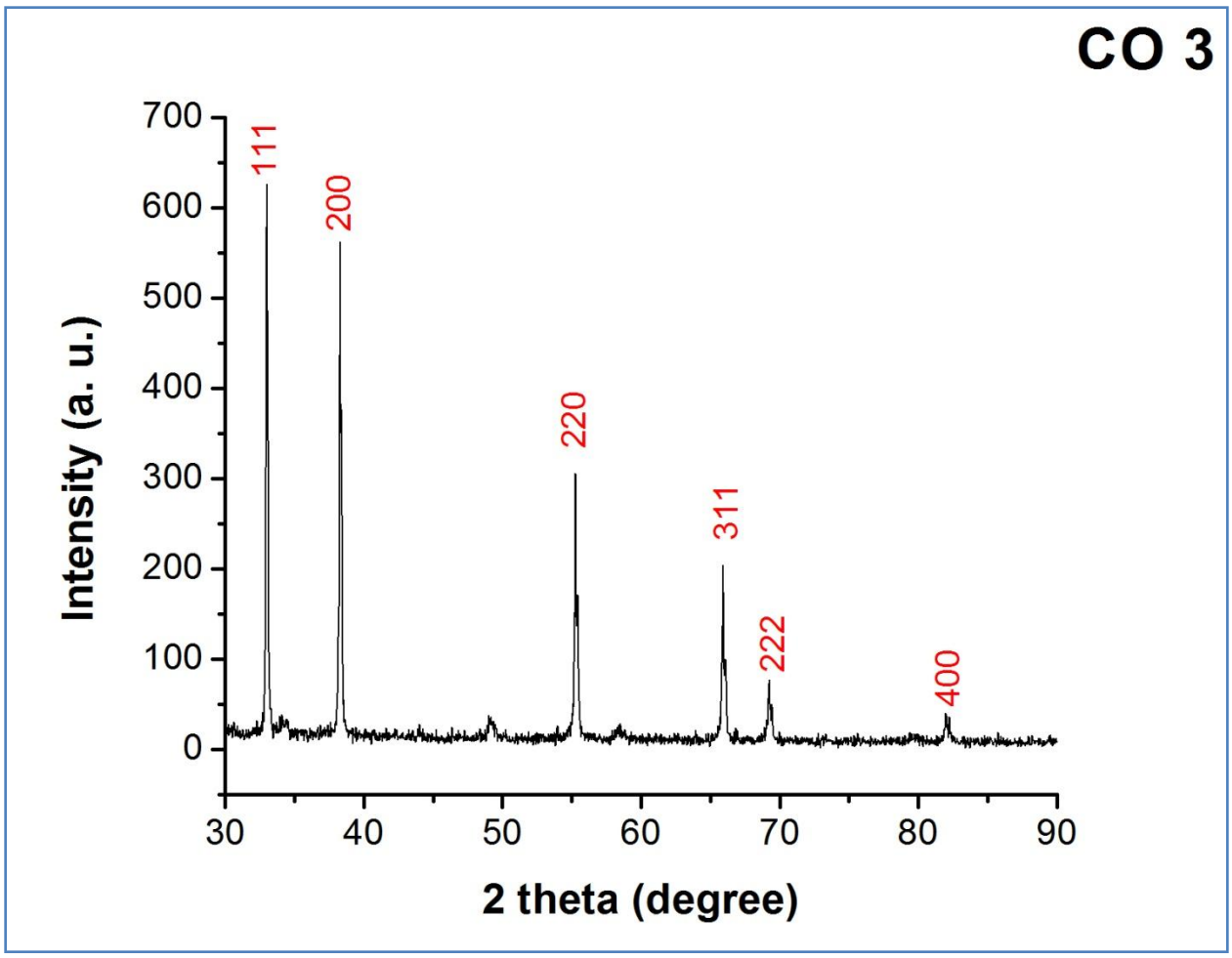


Figure 3.18: XRD pattern of CdO phosphors doped with Yb and Er (CO 3)

Comparison of standard d-values of JCPDS file no. 75 – 0594 with the calculated d-values of the samples are given in table 3.3. The slight deviation from the standard values can be attributed to the presence of activator and co-activator.

| **d – values JCPDS file no. 05 – 0640** | **d – values (Calculated)** | | | | | |
|---|---|---|---|---|---|---|
| | **Sample C 1** | **hkl** | **Sample C 2** | **hkl** | **Sample C 3** | **hkl** |
| 2.712 | 2.7151 | 111 | 2.7151 | 111 | 2.7115 | 111 |
| 2.349 | 2.3484 | 200 | 2.3460 | 200 | 2.3449 | 200 |
| 1.661 | 1.6681 | 220 | 1.6670 | 220 | 1.6697 | 220 |
| 1.416 | 1.4143 | 311 | 1.4135 | 311 | 1.4154 | 311 |
| 1.355 | 1.3541 | 222 | 1.3534 | 222 | 1.3560 | 222 |
| 1.174 | 1.1736 | 400 | 1.1741 | 400 | 1.1749 | 400 |

Table 3.3: Comparison of standard d-values of JCPDS file no. 75 – 0594 with the calculated d-values of the samples of CdO

In case of these samples, no peaks have been observed for $Yb_2O_3$ and $Er_2O_3$, which suggests that Yb and Er have been appropriately incorporated in to the system.

### *3.2.2 Crystallite Size*

The average crystallite size was calculated by Debye – Scherrer formula. The values are given in Table 3.4, 3.5 and 3.6. The results clearly indicate that the samples are in bulk form.

| Sample Name | Crystallite Size (nm) |
|---|---|
| LMO 1 | 61.79 |
| LMO 2 | 69.13 |
| LMO 3 | 74.07 |

Table 3.4: Crystallite size for samples of $La_2(MoO_4)_3$: Yb, Er

| Sample Name | Crystallite Size (nm) |
|---|---|
| BO 1 | 138.54 |
| BO 2 | 110.70 |
| BO 3 | 100.75 |

Table 3.5: Crystallite size for samples of $Bi_2O_3$: Yb, Er

| Sample Name | Crystallite Size (nm) |
|---|---|
| CO 1 | 47.70 |
| CO 2 | 60.06 |
| CO 3 | 73.43 |

Table 3.6: Crystallite size for samples of CdO: Yb, Er

### *3.2.3 SEM analysis*

The scanning Electron Microscopy of the samples were carried out on a JEOL SEM Model JSM 5610, operated on 20 kV. The images were taken at three different resolutions for each sample.

#### *1) $La_2(MoO_4)_3$: $Yb^{3+}$, $Er^{3+}$*

The images for sample LMO 1 are given in figures 3.19 (a), 3.19 (b) and 3.19 (c). The images shows coarse grain structure with a large variation of grain size and aggregation.

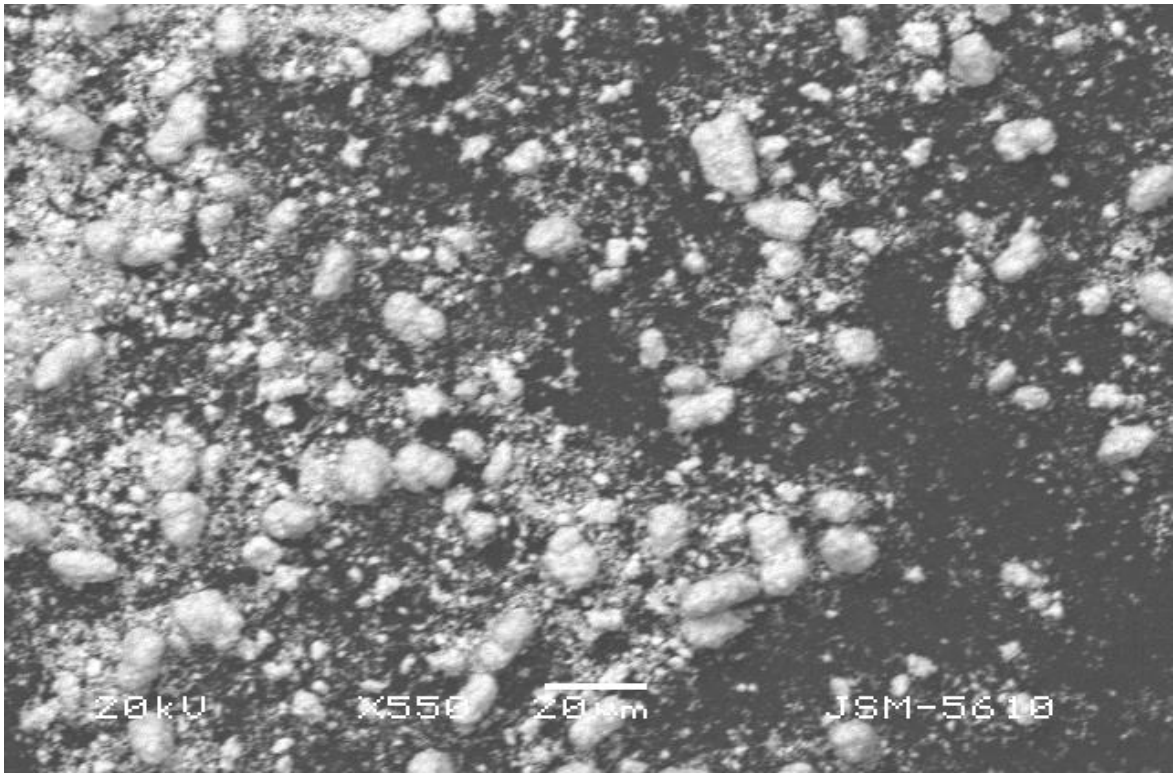


Figure 3.19 (a): SEM image of sample LMO 1 at 550 X

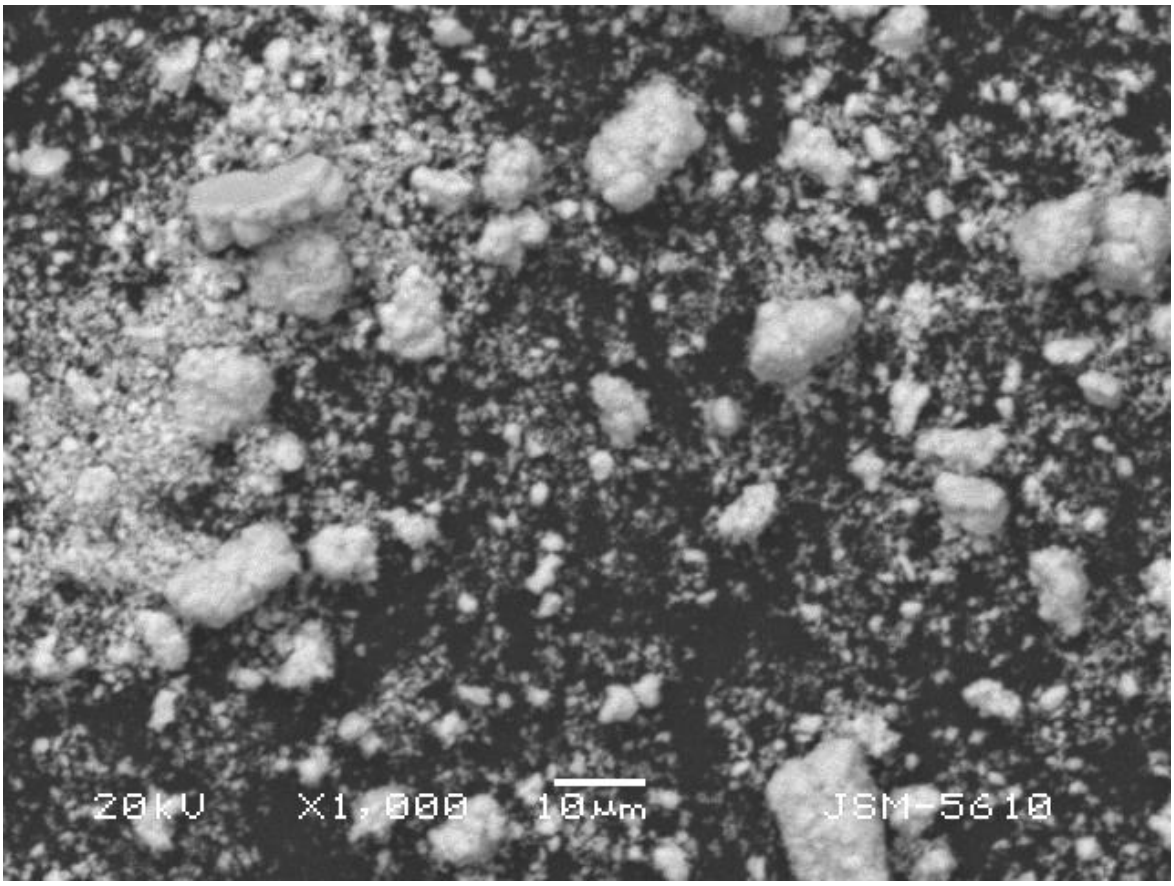


Figure 3.19 (b): SEM image of sample LMO 1 at 1000 X

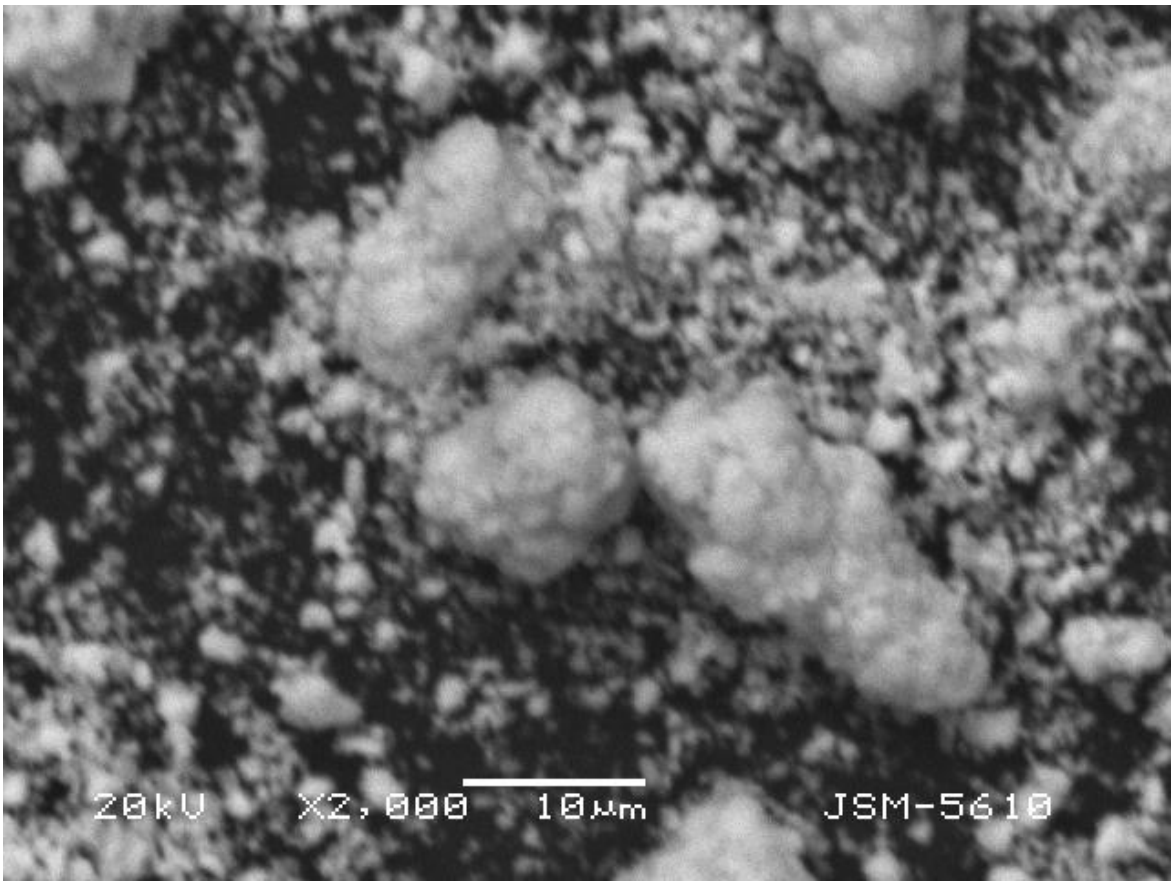


Figure 3.19 (c): SEM image of sample LMO 1 at 2000 X

The images of sample LMO 2 are given in figures 3.20 (a), 3.20 (b) and 3.20 (c). They show the formation of some rod like structures, which become evident as the resolution increases. In these images, large chunks can be seen which look like aggregated grains of rod like structures.

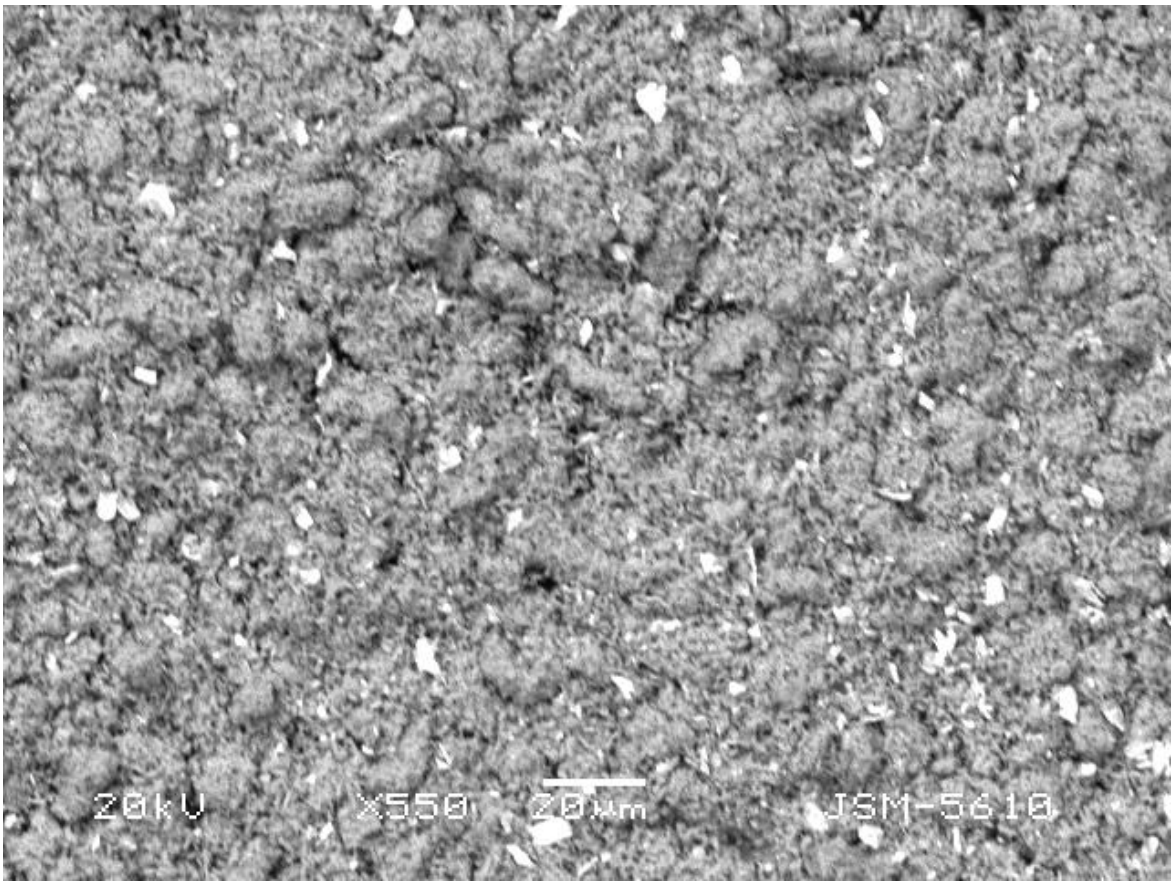


Figure 3.20 (a): SEM image of sample LMO 2 at 550 X

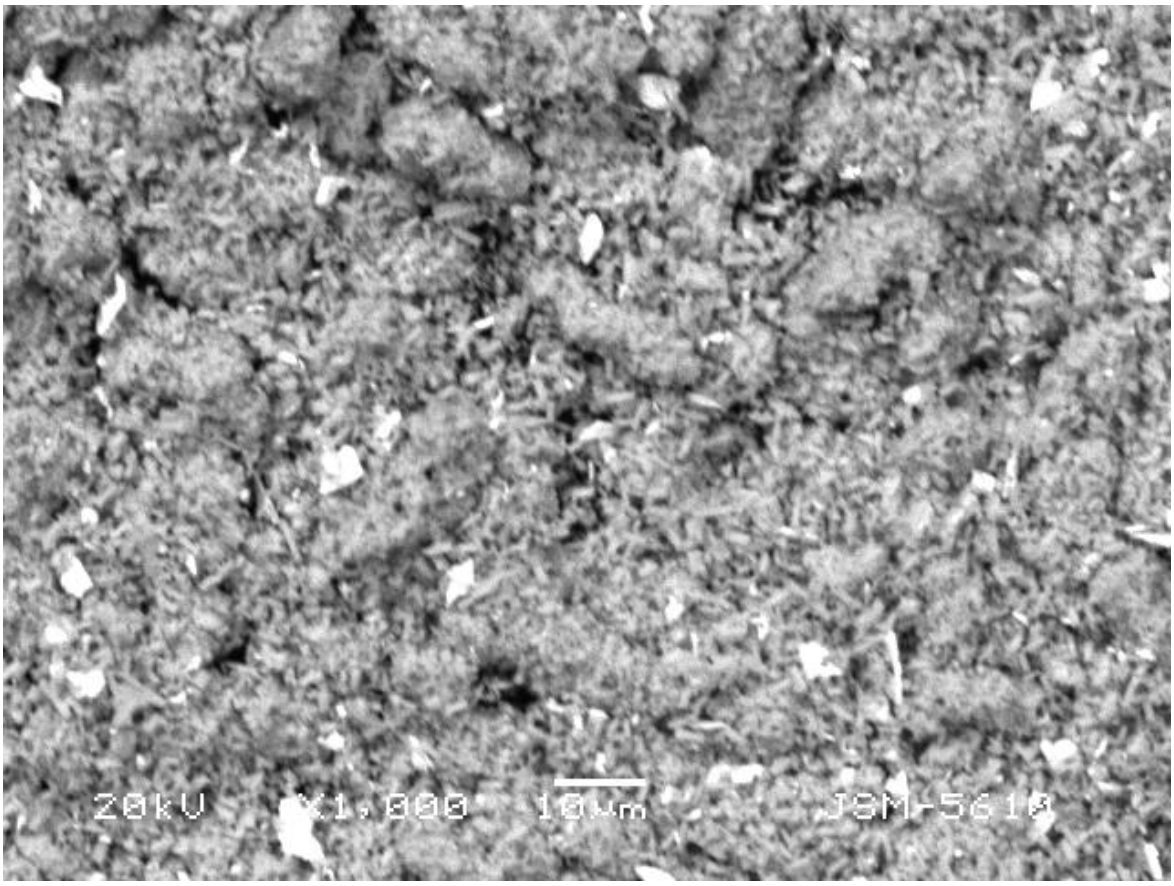


Figure 3.20 (b): SEM image of sample LMO 2 at 1000 X

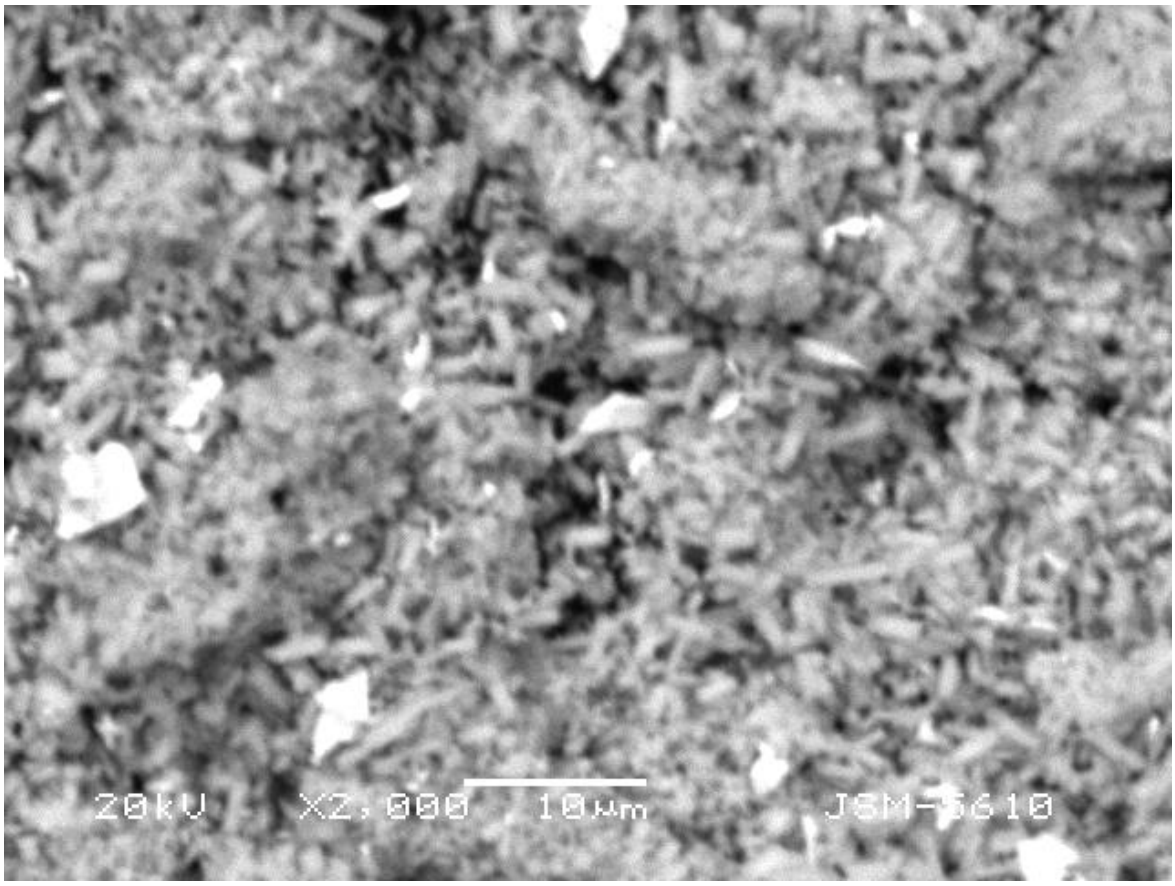


Figure 3.20 (c): SEM image of sample LMO 2 at 2000 X

For images of sample LMO 3 given in figures 3.21 (a), 3.21 (b) and 3.21 (c), the rod structure is further evident. The size distribution does not look to be very wide.

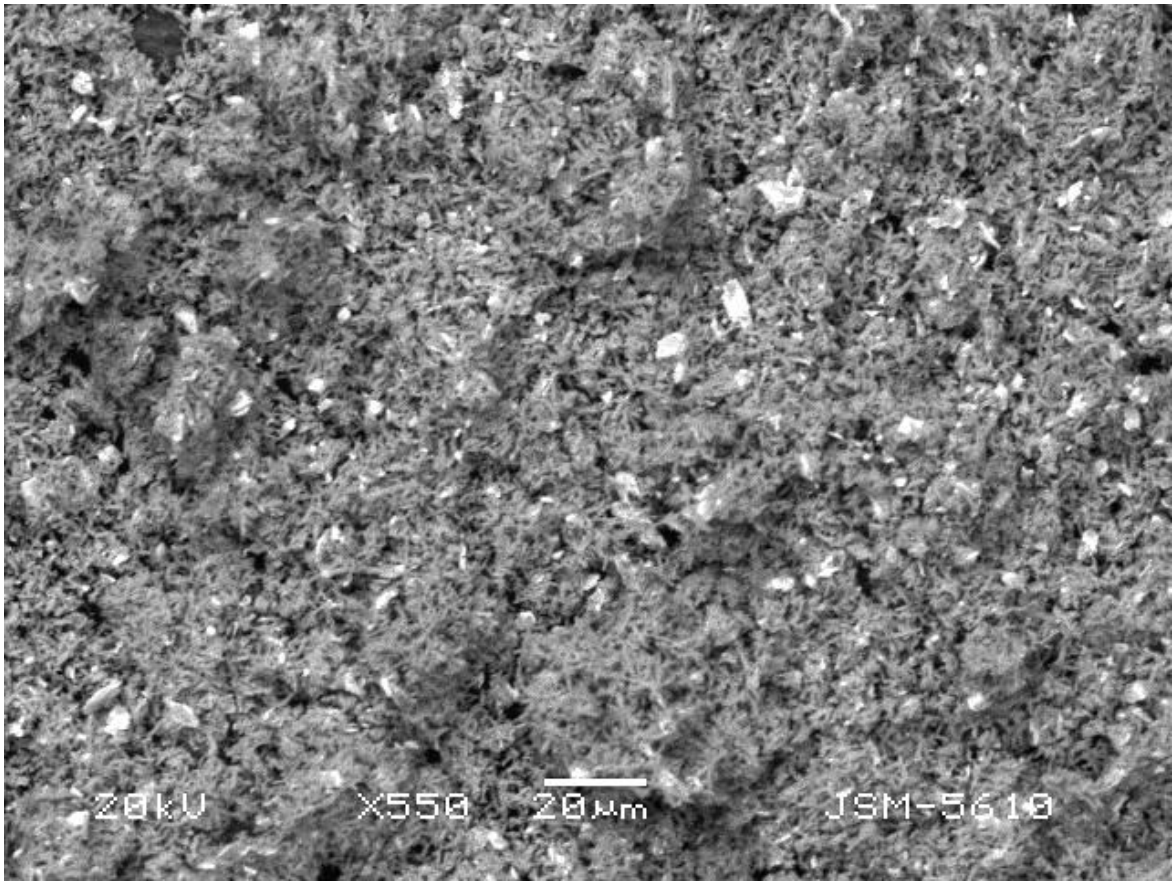


Figure 3.21 (a): SEM image of sample LMO 3 at 550 X

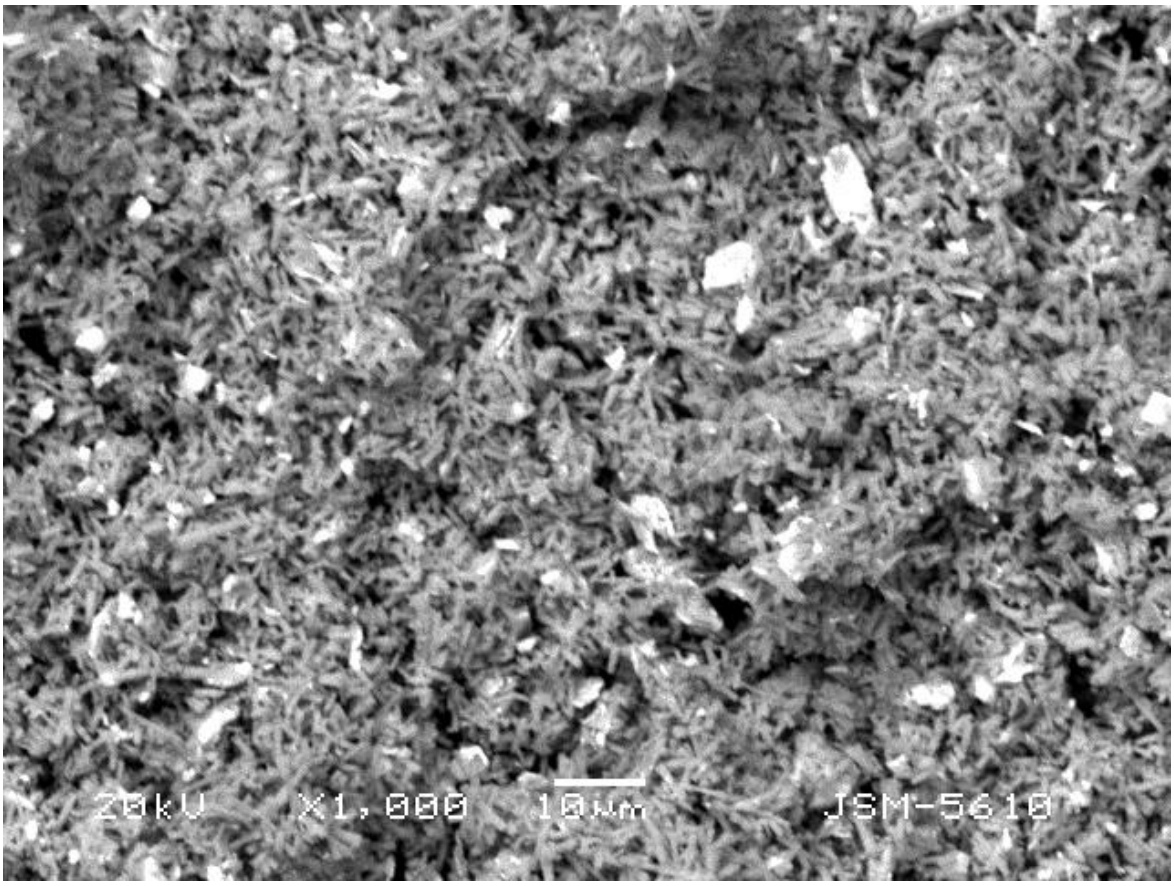


Figure 3.21 (b): SEM image of sample LMO 3 at 1000 X

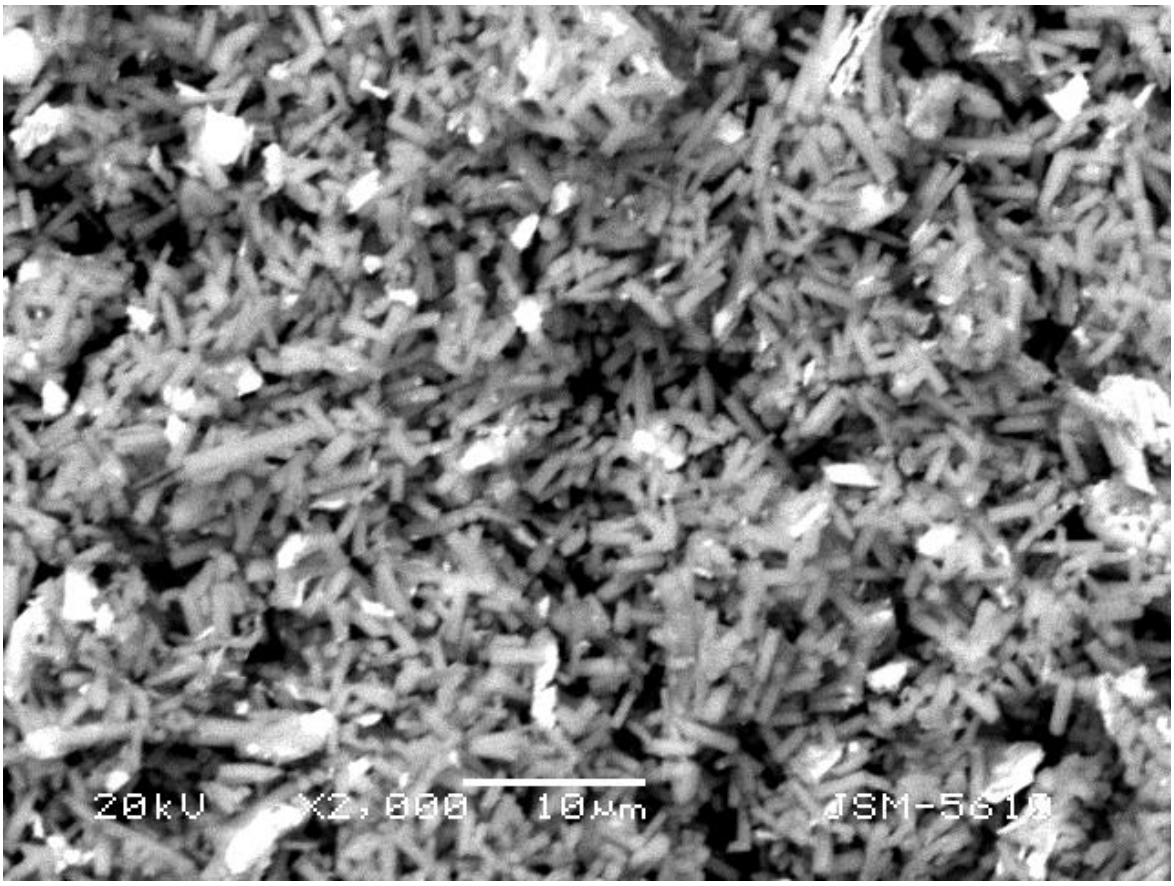


Figure 3.21 (c): SEM image of sample LMO 3 at 2000 X

The difference between the samples LMO 1, LMO 2 and LMO 3 is the amount of Erbium, which increases from LMO 1 to LMO 3. Hence, it can be suggested that the presence of Erbium instrumental in the samples acquiring the rod shape. However, the host material also plays a role in determining the shape. It is also guided by the method of synthesis.

## 2) $Bi_2O_3$: $Yb^{3+}$, $Er^{3+}$

The images (i) for sample BO 1 are given in figures 3.22 (a), 3.22 (b) and 3.22 (c) (ii) for sample BO 2 are given in figures 3.23 (a), 3.23 (b) and 3.23 (c) and (iii) for sample BO 3 are given in figures 3.24 (a), 3.24 (b) and 3.24 (c) respectively.

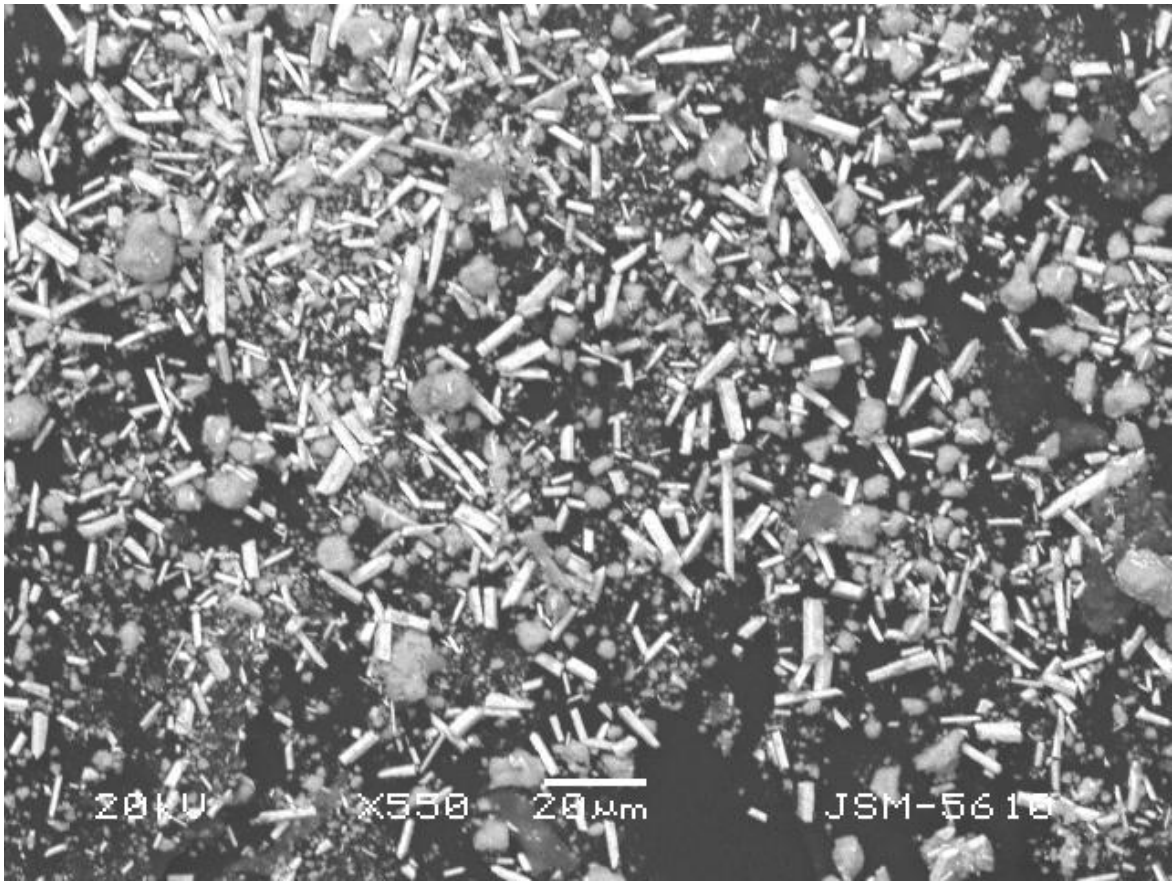


Figure 3.22 (a): SEM image of sample BO 1 at 550 X

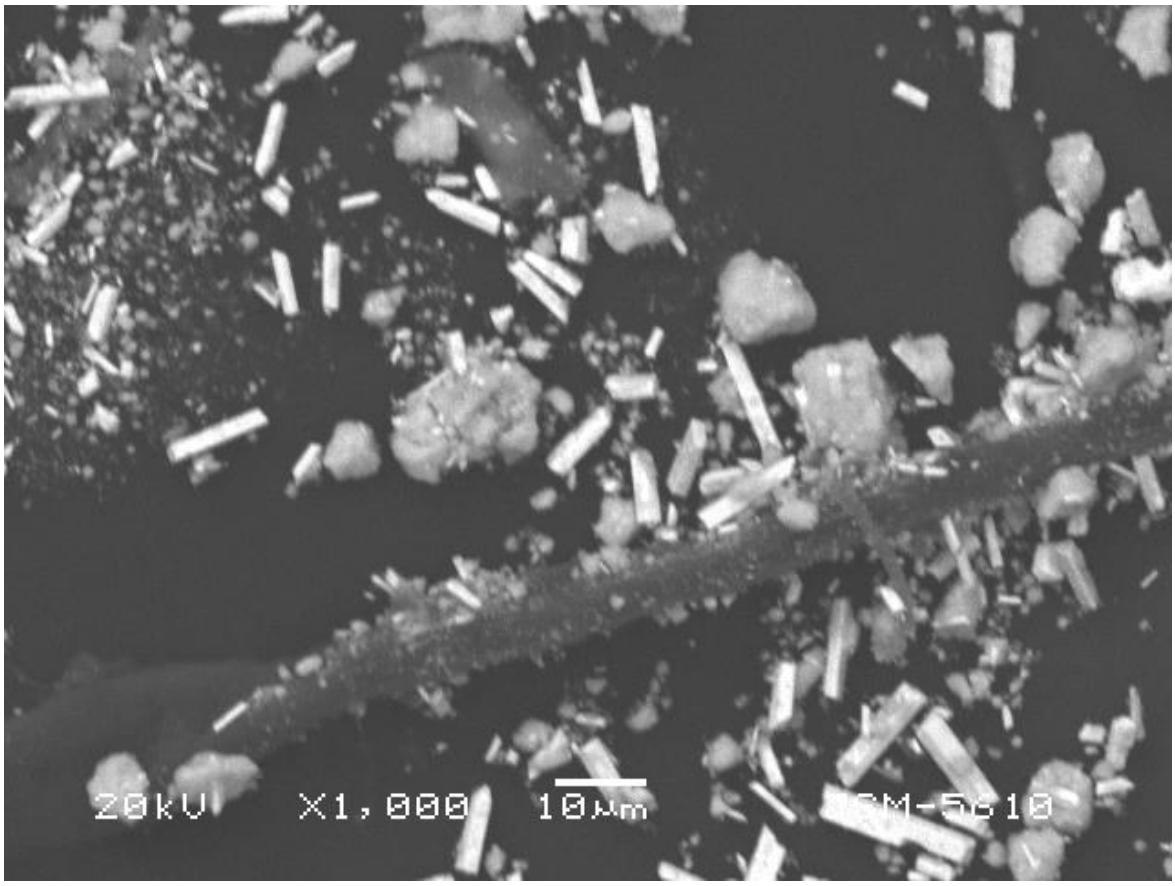


Figure 3.22 (b): SEM image of sample BO 1 at 1000 X

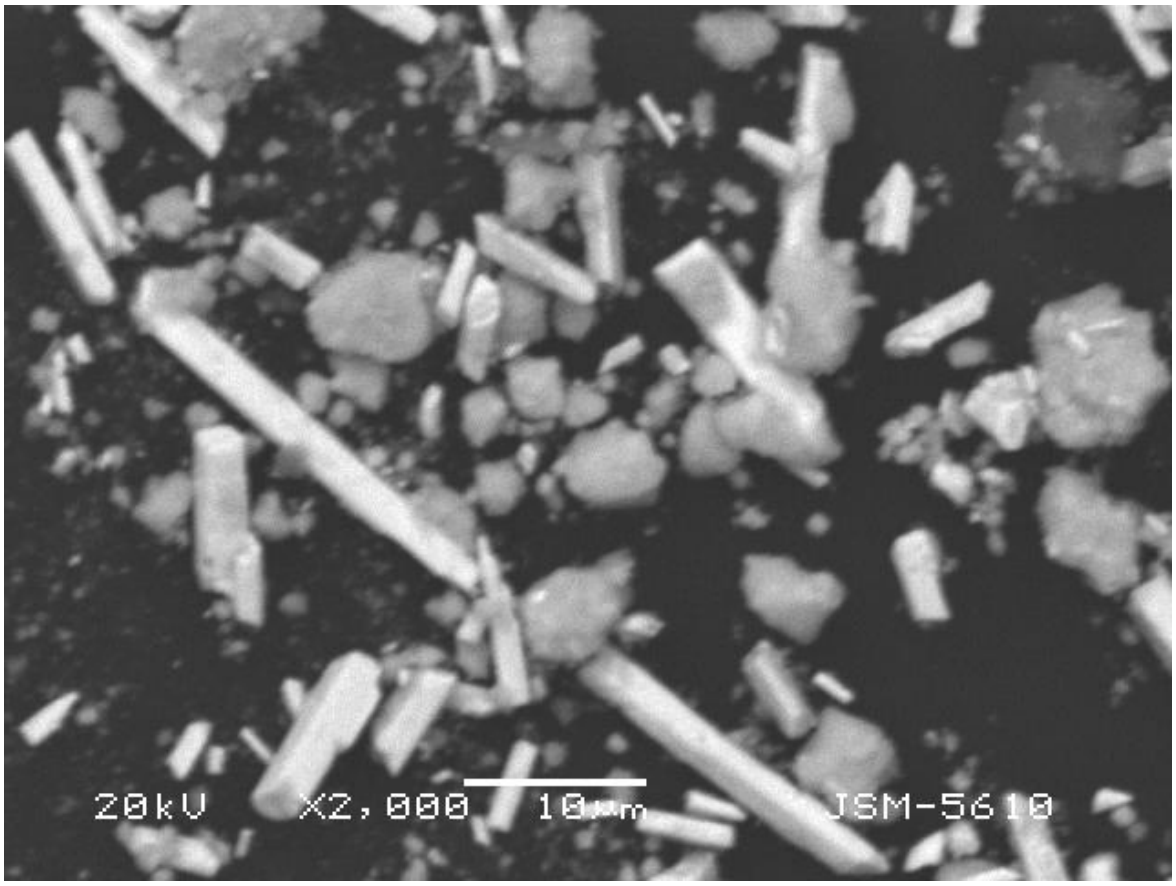


Figure 3.22 (c): SEM image of sample BO 1 at 2000 X

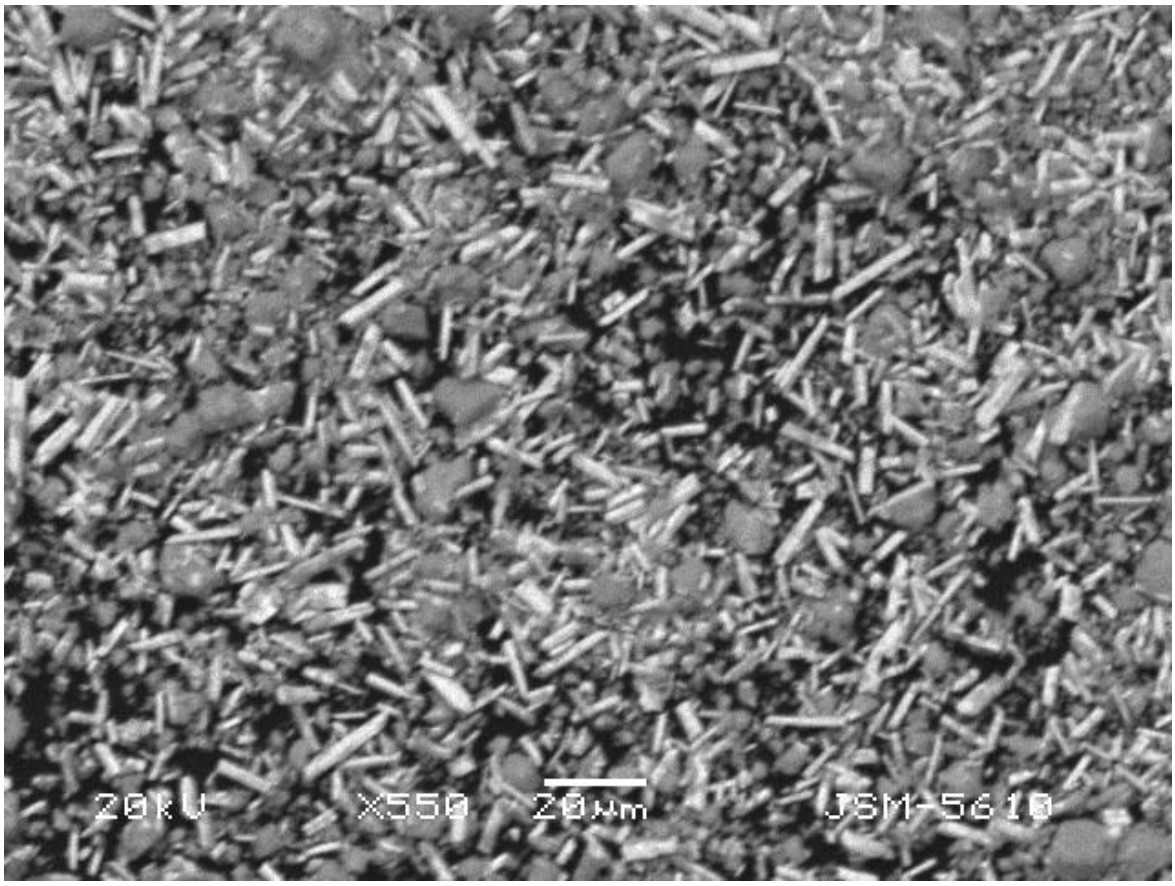


Figure 3.23 (a): SEM image of sample BO 2 at 550 X

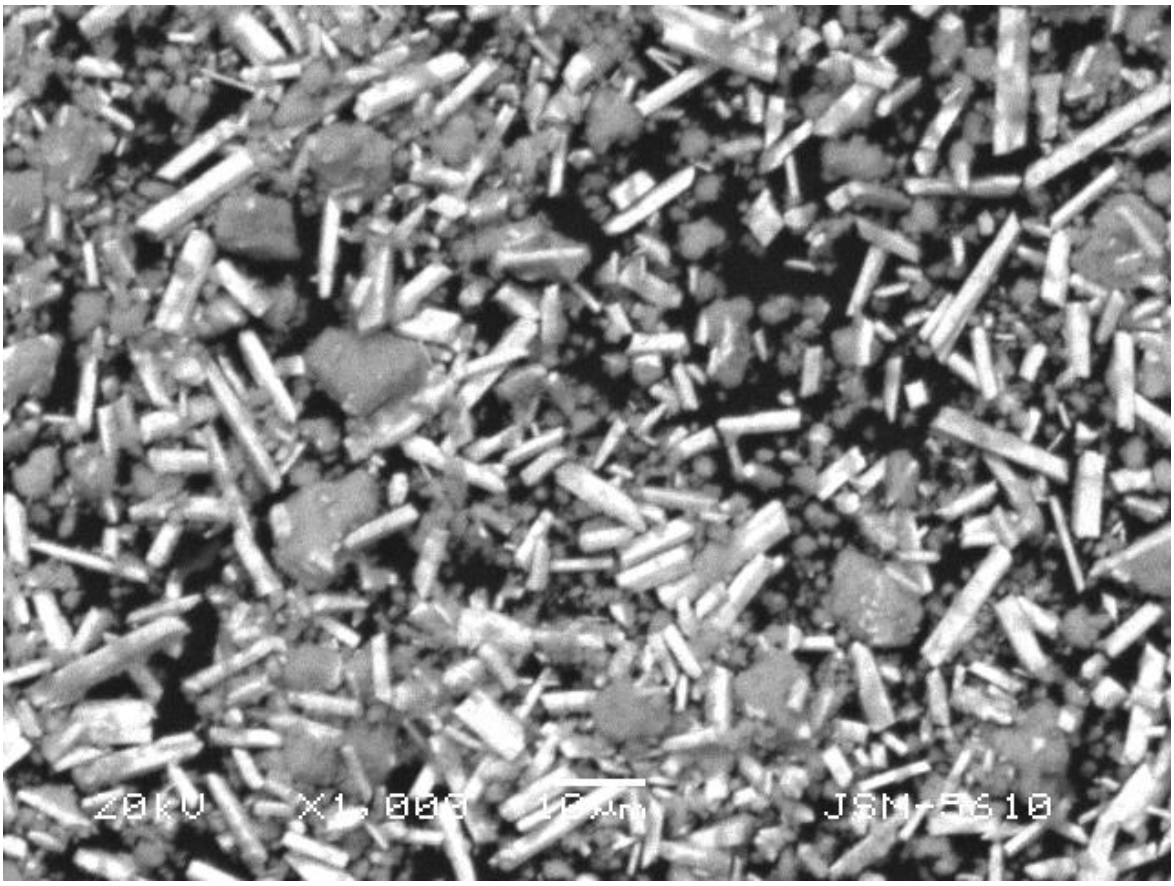


Figure 3.23 (b): SEM image of sample BO 2 at 1000 X

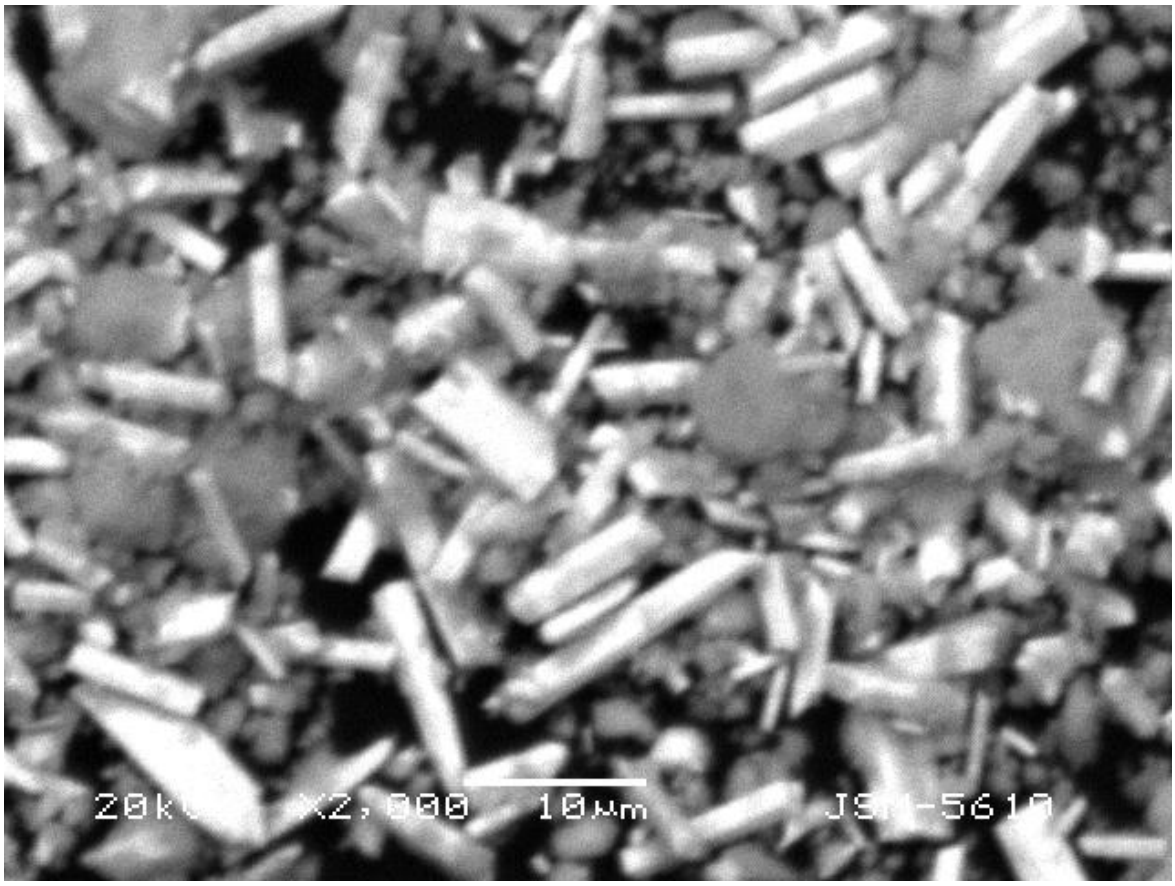


Figure 3.23 (c): SEM image of sample BO 2 at 2000 X

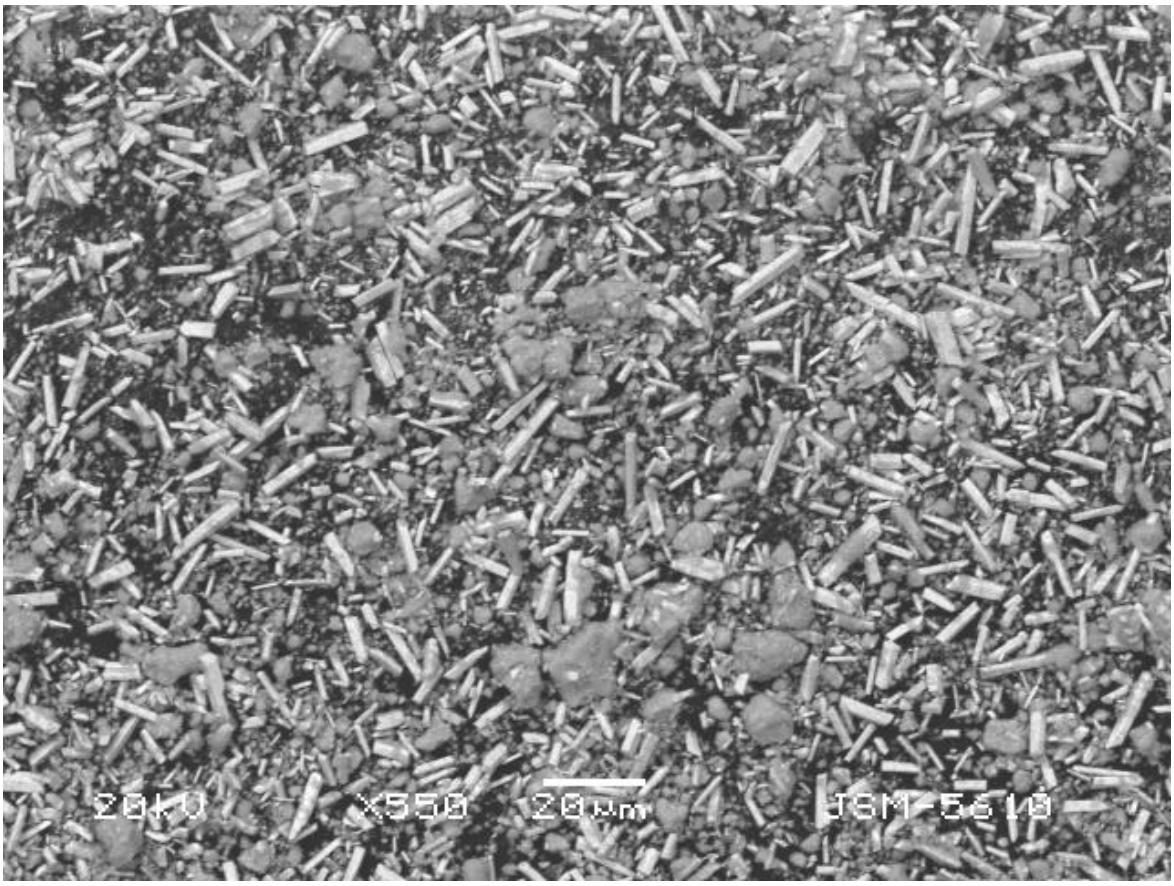


Figure 3.24 (a): SEM image of sample BO 3 at 550 X

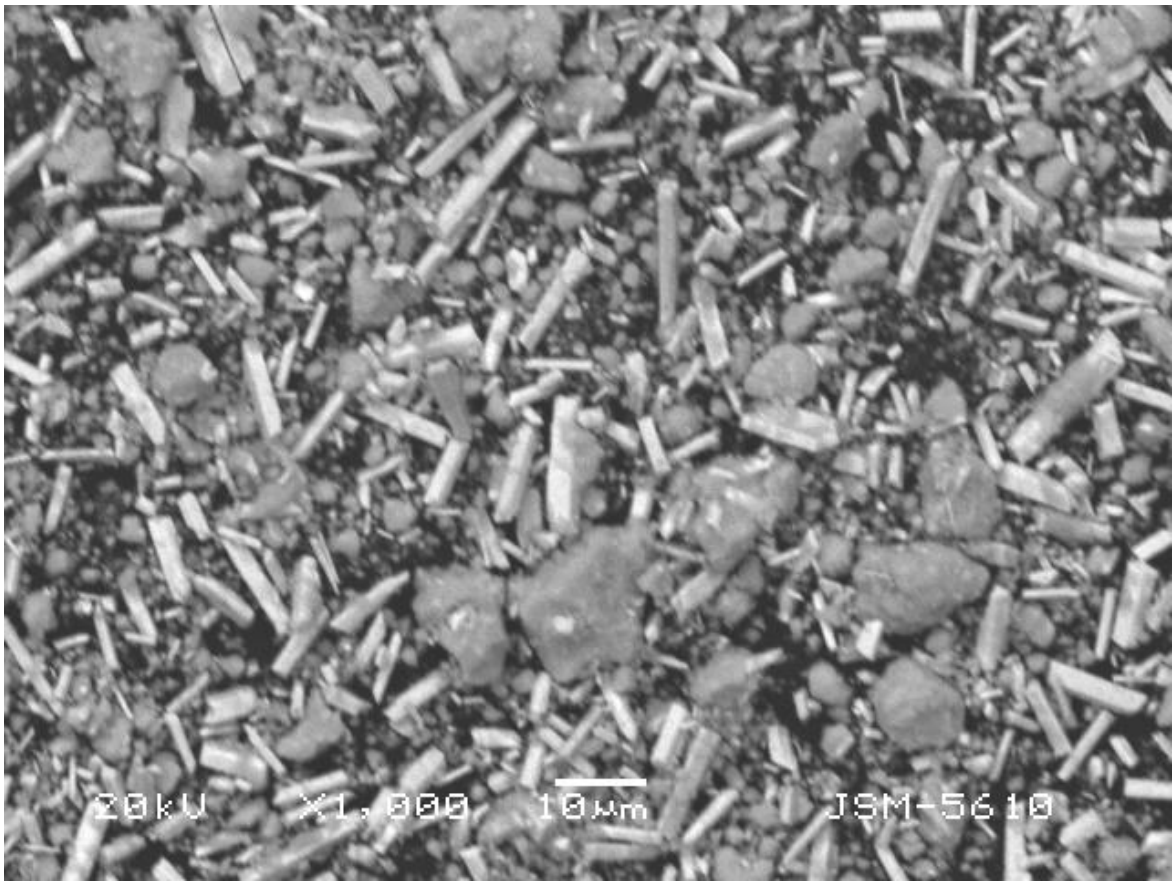


Figure 3.24 (b): SEM image of sample BO 3 at 1000 X


Figure 3.24 (c): SEM image of sample BO 3 at 2000 X

In all the images of samples BO 1, BO 2 and BO 3, there is a mix of coarse grains of varying size and clear rod shaped structures. These rods have a rectangular shape with varying length and width. Some plate like structures can be also seen, particularly at high resolution.

3) ***CdO: $Yb^{3+}$, $Er^{3+}$***

The images (i) for sample CO 1 are given in figures 3.25 (a), 3.25 (b) and 3.25 (c) (ii) for sample CO 2 are given in figures 3.26 (a), 3.26 (b) and 3.26 (c) and (iii) for sample CO 3 are given in figures 3.27 (a), 3.27 (b) and 3.27 (c) respectively.

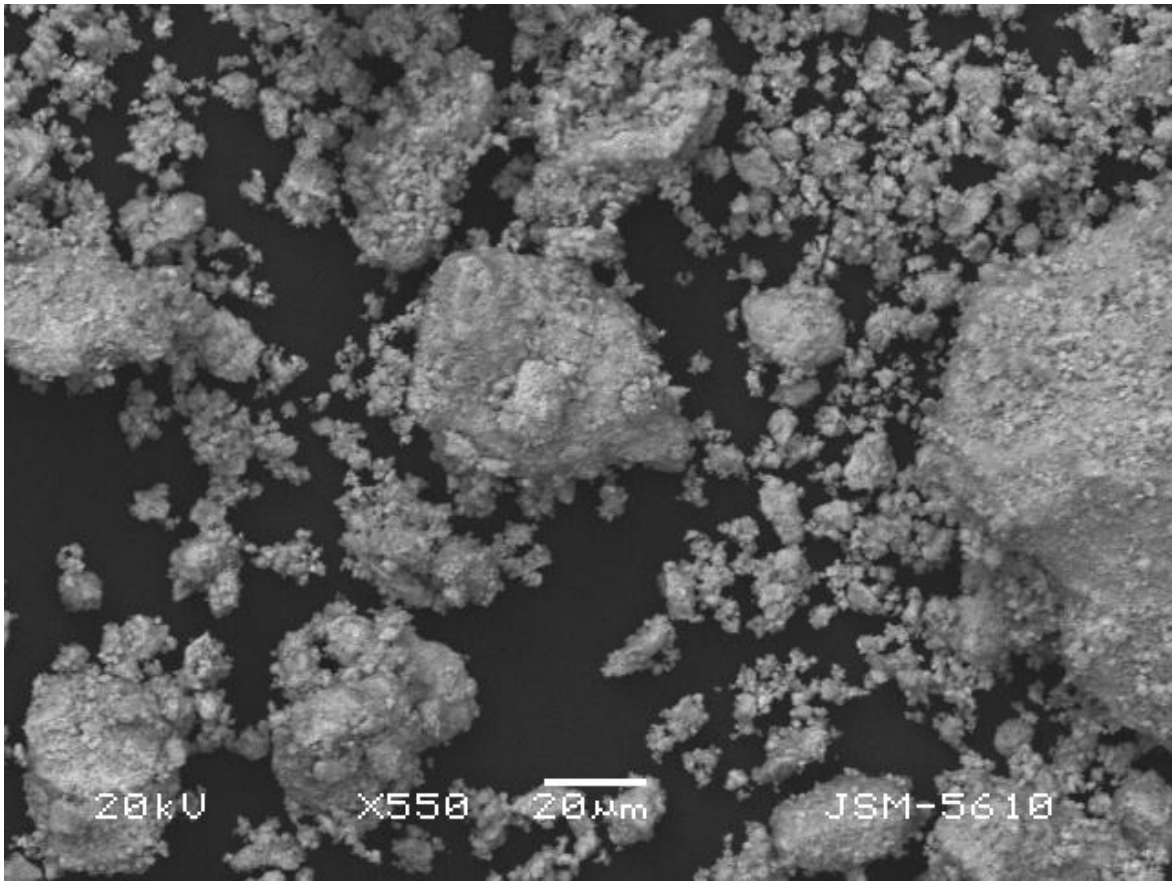


Figure 3.25 (a): SEM image of sample CO 1 at 550 X

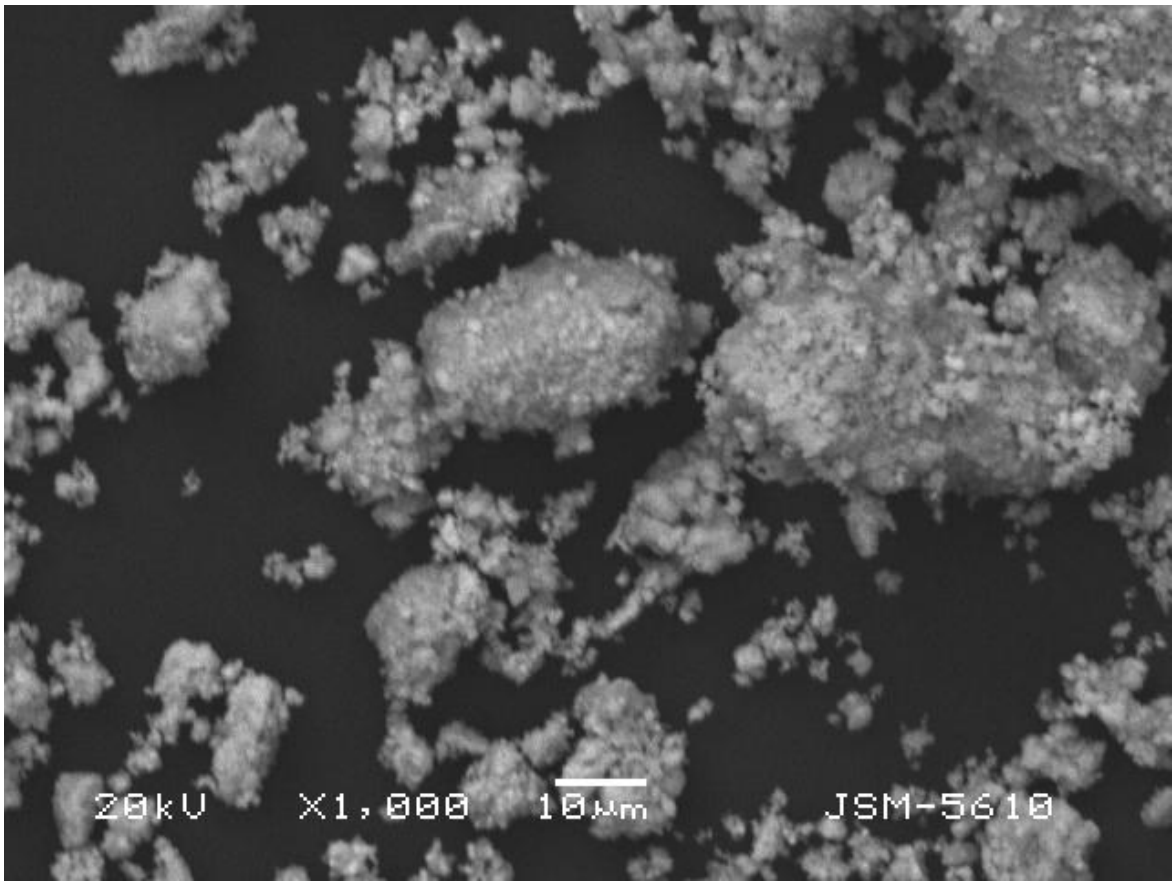


Figure 3.25 (b): SEM image of sample CO 1 at 1000 X

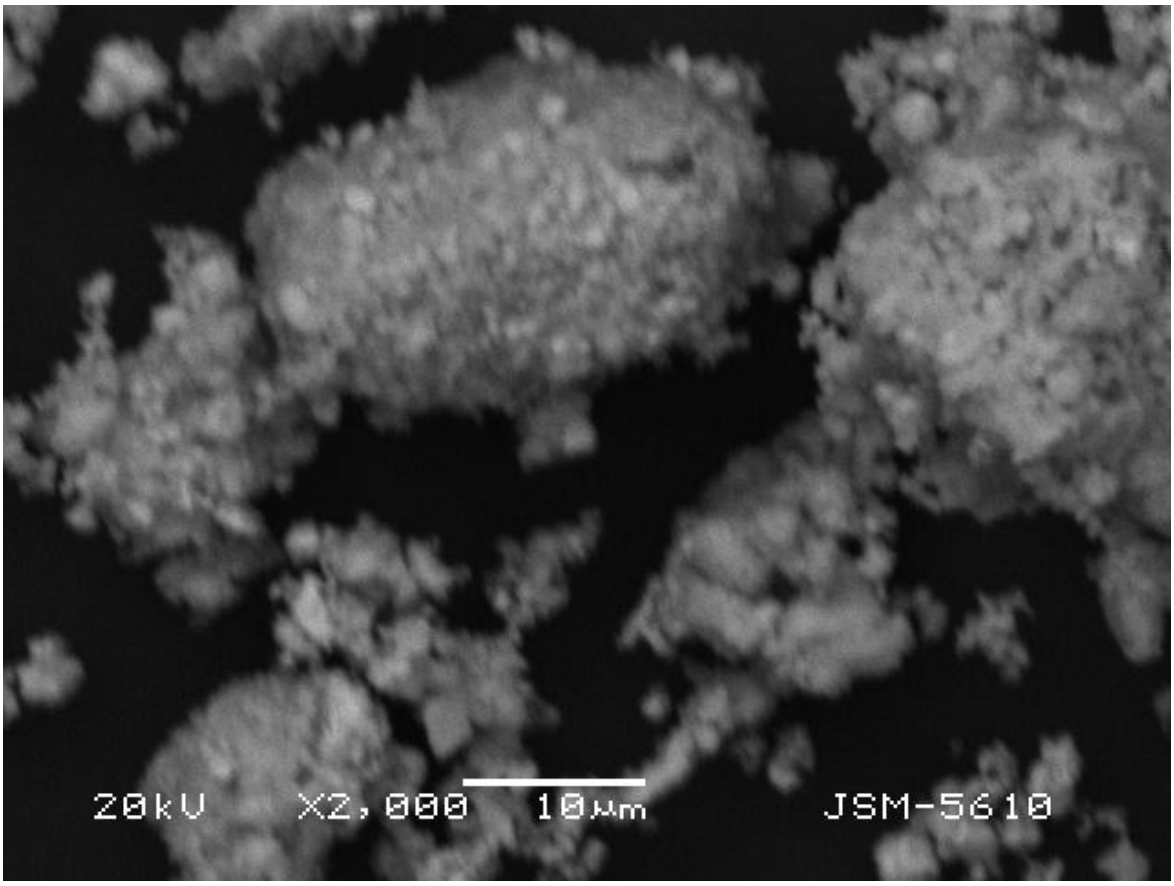


Figure 3.25 (c): SEM image of sample CO 1 at 2000 X

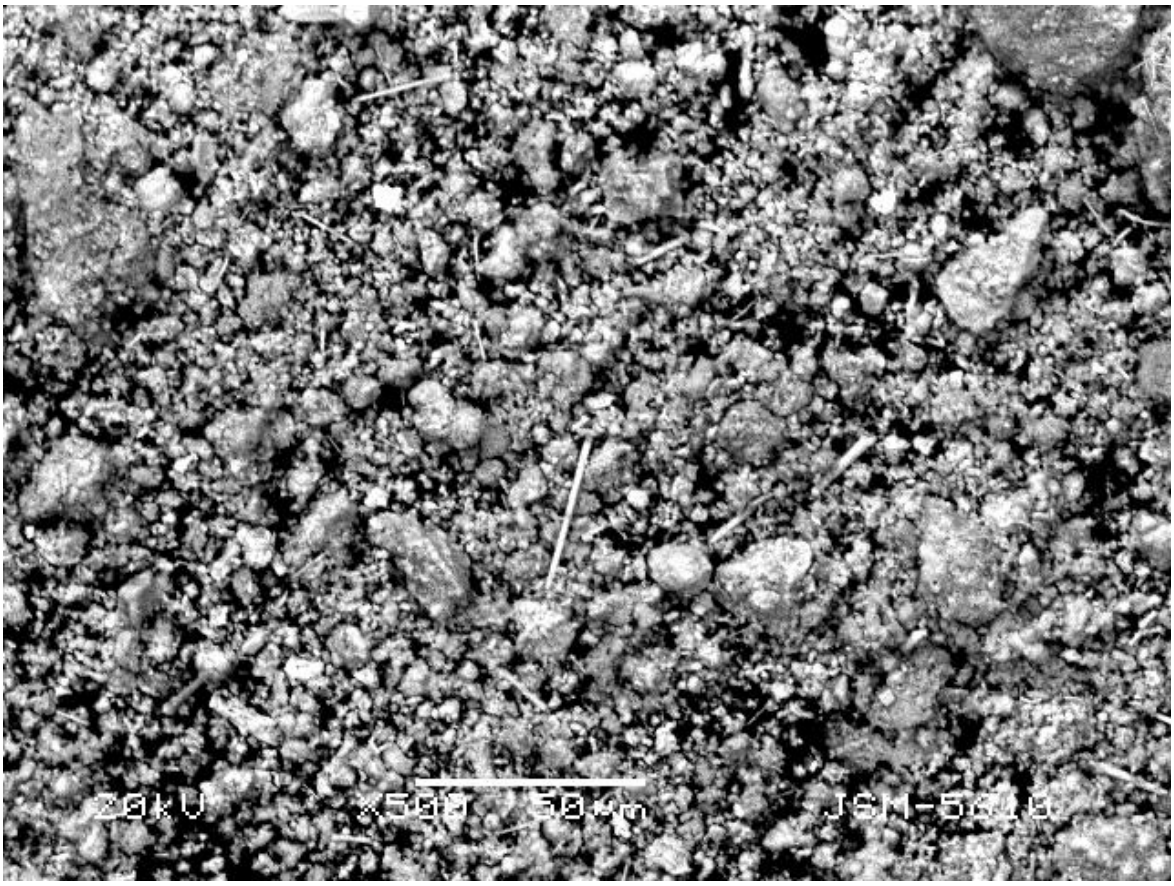

Figure 3.26 (a): SEM image of sample CO 2 at 550 X


Figure 3.26 (b): SEM image of sample CO 2 at 1000 X


Figure 3.26 (c): SEM image of sample CO 2 at 2000 X

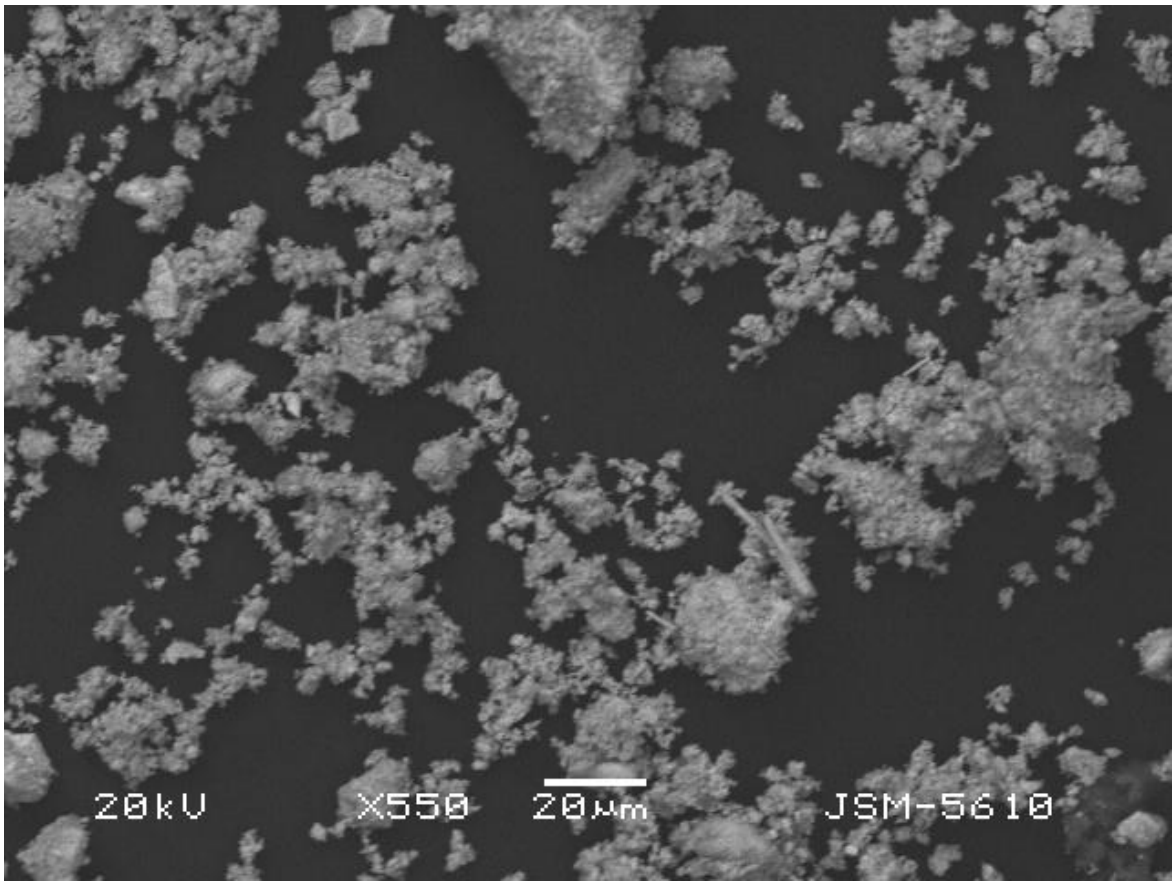


Figure 3.27 (a): SEM image of sample CO 3 at 550 X

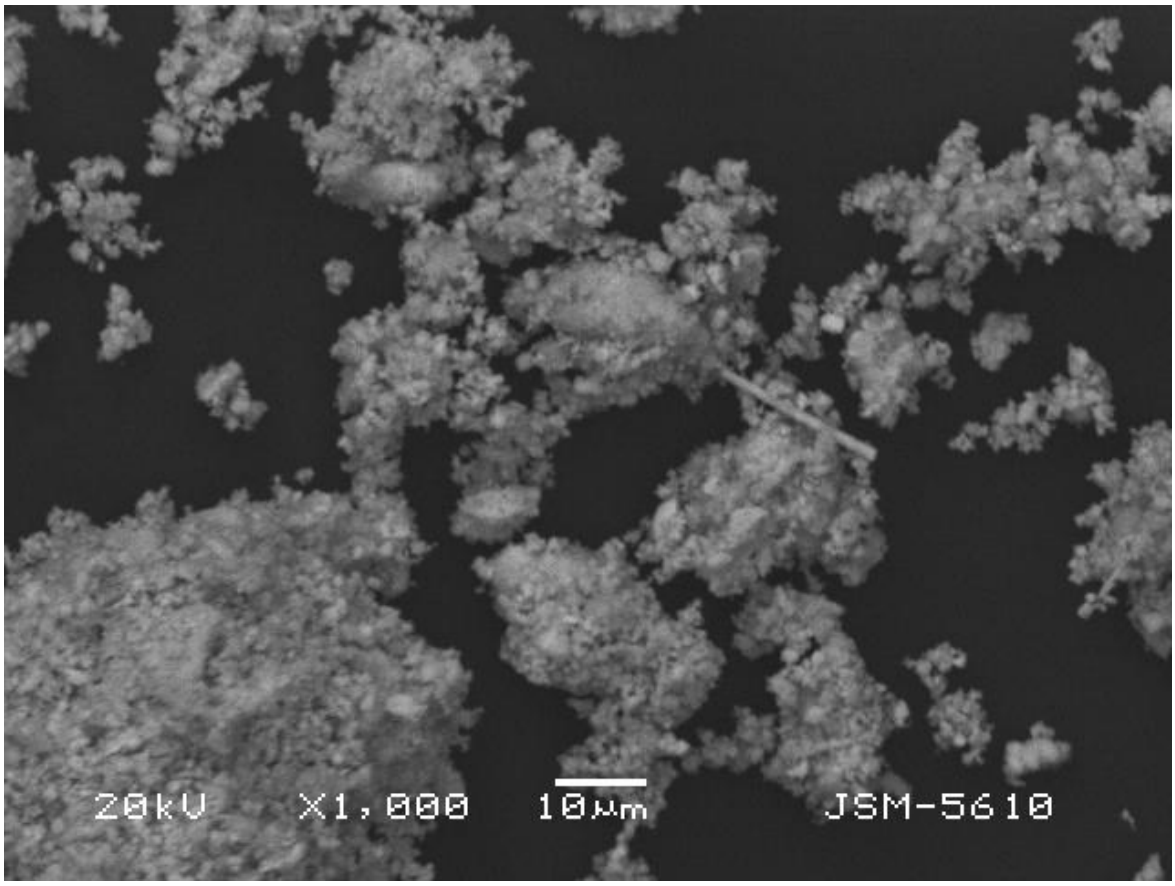


Figure 3.27 (b): SEM image of sample CO 3 at 1000 X

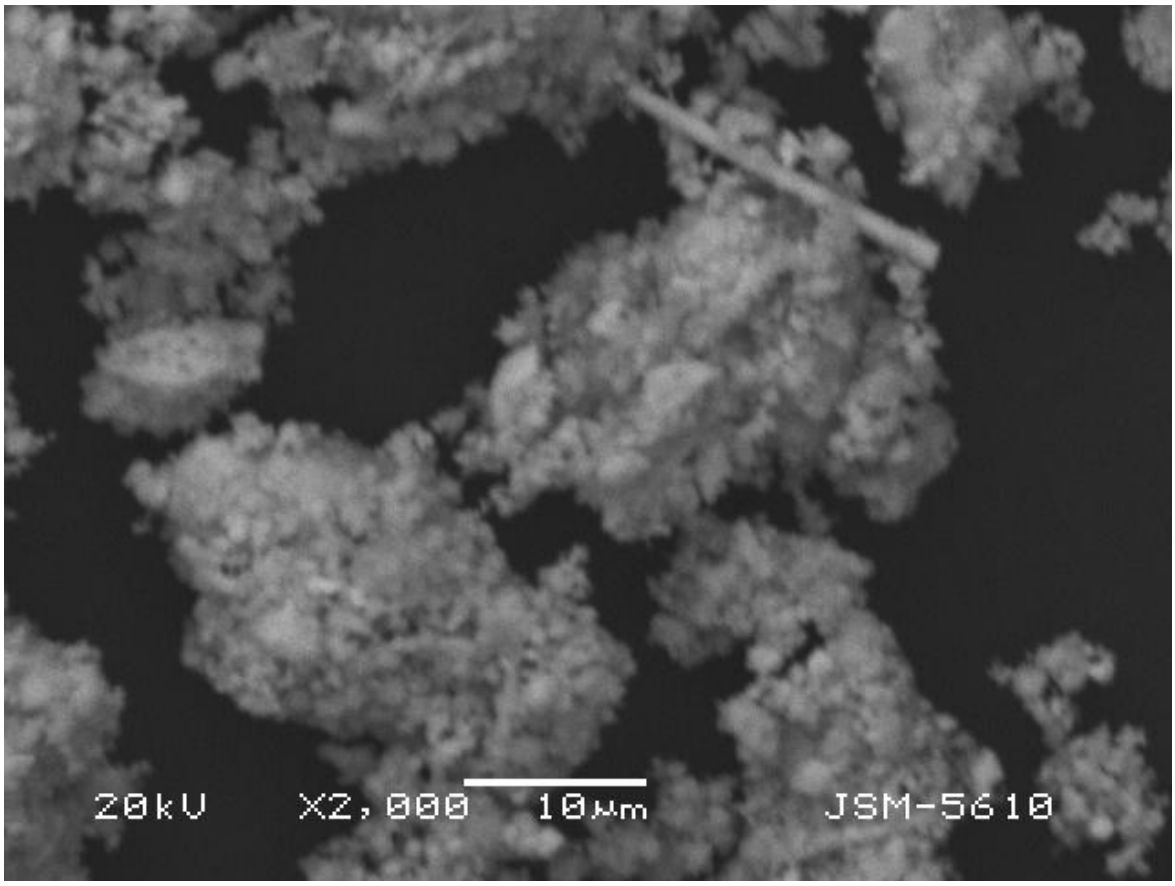


Figure 3.27 (c): SEM image of sample CO 3 at 2000 X

The images of samples CO 1, CO 2 and CO 3 in general show a coarse grain structure with large grains which are aggregates of smaller grains. Samples CO 2 and CO 3 show a few distinct rod structures. However, sample CO 1 does not show any such rods. It is significant that the EDAX analysis shows absence of Er in sample CO 1.

## *3.3 Summary*

The choice of host and activator/sensitizer plays an important role in the performance of a phosphor. Three host materials were chosen for synthesis with $Yb^{3+}$ and $Er^{3+}$ as the sensitizer and activator. These host materials are Lanthanum Molybdate, Bismuth Oxide and Cadmium Oxide. The amount of Ytterbium was kept constant while amount of Erbium was varied. Three samples were prepared for each of the hosts. The samples were prepared using precipitation method.

EDAX analysis of the samples confirms the presence of the activator and sensitizer as well as all elements of the host matrix.

XRD of the Lanthanum Molybdate samples shows that the samples have high degree of crystallinity. They are in monoclinic phase. Samples of Bismuth Oxide also show high degree of crystallinity. They are also in monoclinic phase. Results for Cadmium Oxide samples are similar. They are in cubic phase.

The average crystallite size of the samples is on the higher side. $Bi_2O_3$ samples have the highest size while CdO samples have the lowest.

SEM images of $La_2(MoO_4)_3$ show coarse grain structure with large variation in grain size. Higher resolution images show aggregation of rod like structures. Images of $Bi_2O_3$ samples clearly show rectangular rod structures of different size. Images of CdO sample exhibit coarse grain structure with a few occassional rods.